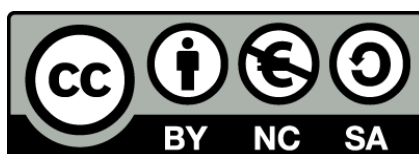




UNIVERSITAT_{DE}
BARCELONA

Nuclear Receptors and c-JUN NH2-Terminal Kinase: Crosstalk and Actions

Carles Bayod Giron



Aquesta tesi doctoral està subjecta a la llicència **Reconeixement- NoComercial – Compartir Igual 4.0. Espanya de Creative Commons.**

Esta tesis doctoral está sujeta a la licencia **Reconocimiento - NoComercial – Compartir Igual 4.0. España de Creative Commons.**

This doctoral thesis is licensed under the **Creative Commons Attribution-NonCommercial-ShareAlike 4.0. Spain License.**



UNIVERSITAT DE
BARCELONA

Unitat de Bioquímica i Biologia Molecular
Departament de Bioquímica i Fisiologia

Facultat de Farmàcia i Ciències de l'Alimentació

UNIVERSITAT DE BARCELONA

**NUCLEAR RECEPTORS AND c-JUN NH₂-TERMINAL KINASE:
CROSSTALK AND ACTIONS**

Carles Bayod Giron, 2020



UNIVERSITAT DE
BARCELONA

Unitat de Bioquímica i Biologia Molecular
Departament de Bioquímica i Fisiologia

Facultat de Farmàcia i Ciències de l'Alimentació

UNIVERSITAT DE BARCELONA

Programa de doctorat de Biomedicina
Any 2020

**NUCLEAR RECEPTORS AND c-JUN NH₂-TERMINAL KINASE:
CROSSTALK AND ACTIONS**

Memòria presentada per Carles Bayod Giron per optar al títol de doctor
per la Universitat de Barcelona.

Dra. Carme Caelles Franch

Carles Bayod Giron

Carles Bayod Giron, 2020

I have not failed. I've just found 10.000 ways that won't work.

Thomas A. Edison

ABBREVIATIONS

ABCA1	ATP-BINDING CASSETTE SUBFAMILY A MEMBER 1
ABCG1	ATP-BINDING CASSETTE SUBFAMILY G MEMBER 1
AF	ACTIVATION FUNCTION
AP-1	ACTIVATOR PROTEIN 1
AR	ANDROGEN RECEPTOR
ASK	APOPTOSIS SIGNAL-REGULATED KINASE
BAT	BROWN ADIPOSE TISSUE
ChREBP	CARBOHYDRATE RESPONSE ELEMENT-BINDING PROTEIN
CMC	CARBOXYMETHYL CELLULOSE
DMF	DIMETHYLFORMAMIDE
DUSP	DUAL SPECIFICITY PHOSPHATASE
ER	ENDOPLASMIC RETICULUM
ERK	EXTRACELLULAR SIGNAL-REGULATED KINASE
ERS	ENDOPLASMIC RETICULUM STRESS
eWAT	EPIDIDYMAL WHITE ADIPOSE TISSUE
FABP4	FATTY ACID-BINDING PROTEIN 4
FDA	FOOD AND DRUG ADMINISTRATION
F-L-Leu	FMOC-L-LEUCINE
GC	GLUCOCORTICOID
GLUT	GLUCOSE TRANSPORTER
GR	GLUCOCORTICOID RECEPTOR
GRE	GLUCOCORTICOID RESPONSE ELEMENT
GSV	GLUT4 STORAGE VESICLES
HDL	HIGH-DENSITY LIPOPROTEIN
HRE	HORMONAL RESPONSE ELEMENTS
HSP	HEAT-SHOCK PROTEIN
IFNγ	INTERFERON GAMMA

Abbreviations

IL-1β	INTERLEUKIN-1 BETA
INSIG-1	INSULIN-INDUCED GENE 1
InsR	INSULIN RECEPTOR
IR	INSULIN RESISTANCE
IRS	INSULIN RECEPTOR SUBSTRATE
JNK	C-JUN N-TERMINAL KINASE
LBD	LIGAND BINDING DOMAIN
LPS	LIPOPOLYSACCHARIDE
LXR	LIVER X RECEPTOR
LXRE	LXR RESPONSE ELEMENT
MAPK	MITOGEN-ACTIVATED PROTEIN KINASE
MAPKAPK	MAPK-ACTIVATED PROTEIN KINASE
MAP2K	MAPK KINASE
MAP3K	MAPKK KINASE
MEF	MOUSE EMBRYONIC FIBROBLASTS
MK	MAPKAPK
MKP	MAPK PHOSPHATASE
MLK	MIXED LINEAGE KINASE
MNK	MAPK-INTERACTING KINASE
MSK	MITOGEN- AND STRESS-ACTIVATED KINASE
NF-κB	NUCLEAR FACTOR KAPPA-LIGHT-CHAIN-ENHANCER OF ACTIVATED B CELLS
NLS	NUCLEAR LOCALISATION SIGNAL
NR	NUCLEAR RECEPTOR
NTD	N-TERMINAL DOMAIN
PEPCK	PHOSPHOENOLPYRUVATE CARBOXYKINASE
PGC-1α	PPAR GAMMA COACTIVATOR-1 ALPHA
PP5	PROTEIN PHOSPHATASE 5

PPAR	PEROXISOME PROLIFERATOR-ACTIVATED RECEPTOR
PPARγ₁	PPAR GAMMA ISOFORM 1
PPARγ₂	PPAR GAMMA ISOFORM 2
PPRE	PPAR RESPONSE ELEMENT
PTM	POST-TRANSLATIONAL MODIFICATION
PUFA	POLYUNSATURATED FATTY ACID
RAR	RETINOID ACID RECEPTOR
ROS	REACTIVE OXYGEN SPECIES
RSK	P90 RIBOSOMAL S6 KINASE
RXR	RETINOID X RECEPTOR
SAPK	STRESS-ACTIVATED PROTEIN KINASE
SCAP	SREBP CLEAVAGE-ACTIVATING PROTEIN
SREBP1	STEROL REGULATORY ELEMENT-BINDING PROTEIN 1C
T2D	TYPE 2 DIABETES
TAK	TGF β -ACTIVATED KINASE
TAO	THOUSAND AND ONE-AMINO ACID KINASE
TG	THAPSIGARGIN
TNFα	TUMOUR NECROSIS FACTOR ALPHA
TPL	TUMOR PROGRESSION LOCUS
TZD	THIAZOLIDINEDIONE
UPR	UNFOLDED PROTEIN RESPONSE
WAT	WHITE ADIPOSE TISSUE

TABLE OF CONTENTS

ABSTRACT	1
INTRODUCTION	3
1. The Nuclear Receptor Superfamily	5
1.1. Nuclear Receptor Structure	5
1.2. Nuclear receptor transcriptional regulation	7
1.3. Glucocorticoid receptor (GR)	9
1.4. Peroxisome proliferator-activated receptor (PPAR)	10
1.5. Liver X Receptor (LXR)	13
1.6. Retinoid X Receptor (RXR)	15
2. Mitogen Activated Protein Kinases (MAPK)	15
2.1. MAPK Regulatory Mechanisms	16
2.2. Stress Activated Protein Kinases (SAPK)	18
3. c-Jun N-terminal Kinase (JNK) – Nuclear Receptor Interaction	20
3.1. JNK – GR	20
3.2. JNK – PPAR γ	23
4. JNK-NR crosstalk: from targeting inflammation to drug resistance	25
4.1. GC therapeutic response	26
4.2. Obesity, Type 2 Diabetes and Inflammation	28
OBJECTIVES	35
MATERIALS AND METHODS	39
1. Cell culture	41
2. <i>In vivo</i> experimental models	41

Table of contents

2.1. Obesity-induced insulin resistance	41
2.2. Glucose and insulin tolerance test	42
2.3. Nuclear receptor agonist treatments	42
3. Genotyping	42
4. Primary cell culture	44
4.1. Bone marrow derived macrophages (BMDM)	44
4.2. Thioglycolate-elicited peritoneal macrophages	45
5. 3T3-L1 adipocyte differentiation	45
6. Transient transfection of pCMV-hINSIG1-Myc	46
7. Murine <i>insig-1</i> knock-down in 3T3-L1 fibroblasts	46
8. Human <i>insig-1</i> stable transfection in HeLa	47
9. Cell extracts and immunoblotting analysis	48
10. Enzyme-Linked Immunosorbent Assay (ELISA)	50
11. JNK immunocomplex assay	50
12. Reverse transcriptase quantitative real-time PCR (RT-qPCR)	51
13. Statistical analysis	53
RESULTS	57
1. To develop an <i>in vivo</i> tool to analyse the effects of the overexpression of JNK in myeloid cells, a very important cell type in early stages of metaflammation and consequently the development of IR	59
1.1. Effects of MKK7D expression on JNK activation and pro-inflammatory gene expression in myeloid cells	60
1.2. mMKK7D mice are not protected from diet-induced obesity or IR	62

2. To analyse whether MKP-1 mediates the insulin sensitizing activity of TZDs	64
2.1. MKP1-KO mice are protected from HFD-induced obesity but not from glucose intolerance or insulin resistance and are responsive to rosiglitazone	64
2.2. Rosiglitazone reduces HFD-induced hyperinsulinemia and has similar effects in InsR pathway in both genotypes	67
3. To analyse whether PP5 mediates the insulin sensitizing activity of LXR agonists	70
3.1. PP5 knockout mice are not protected from diet-induced obesity, glucose intolerance or insulin resistance and did not influence LXR insulin-sensitizing action	70
3.2. PP5 deficiency does not have a differential effect on the insulin-induced activation of the InsR cascade in insulin-target tissues	72
3.3. Obesity-induced JNK activation and its downregulation by the LXR agonist are independent of PP5	74
4. To analyse INSIG-1 as a potential mediator in the crosstalk of PPARγ and LXR with the JNK pathway	76
4.1. Induction of INSIG-1 expression by PPAR γ and LXR activation	76
4.2. INSIG-1 overexpression in HeLa cells downmodulates the JNK activation in response to different stimuli	78
DISCUSSION	83
1. Developing a first-step mouse model to study the effects of JNK activation in myeloid cells	85

Table of contents

2. Rosiglitazone insulin-sensitizing action is not affected by MKP-1-deficiency	88
3. PP5 is not mediating the insulin-sensitizing action of the LXR agonist GW3965	89
4. INSIG-1 is a negative regulator of the JNK cascade	91
CONCLUSIONS	95
REFERENCES	99
ANNEX-I: DIET COMPOSITIONS	119

ABSTRACT

The nuclear receptors (NR) modulate gene transcription in a ligand-dependent manner throughout different mechanisms. A set of NR, including PPAR γ and LXR, are important regulators of carbohydrate and lipid metabolism as well as the immune system. In this regard, both PPAR γ and LXR agonists ameliorate obesity-associated insulin resistance and show anti-inflammatory activity. The c-Jun N-terminal kinase (JNK), a member of the mitogen-activated protein kinases (MAPKs), is also involved in the metabolic and immune system regulation but in contrast to PPAR γ and LXR, JNK activation promotes insulin resistance and triggers the inflammatory response. Due to these opposite actions, an intense and negative crosstalk exists between these NR and the JNK pathway. In this regard, the PPAR γ ligands TZDs perform their insulin sensitizing action through the inhibition of obesity-induced JNK activation. Therefore, in this study we aimed to develop an *in vivo* model for specific activation of JNK in myeloid cells to study PPAR γ and LXR on the JNK-induced inflammatory response. This mouse model was obtained by crossing mice from a transgenic strain generated in our group, which is able to induce the expression of a JNK activator in a Cre recombinase-dependent manner, with the LysMCre mice. In addition, since PPAR γ and LXR interaction with the JNK pathway seems to require transcription, we have tested several PPAR γ and LXR target genes as candidate mediators in this crosstalk.

INTRODUCTION

1. The Nuclear Receptor Superfamily

The human genome codes for 48 members of the nuclear receptor (NR) superfamily, more than twice the amount *Drosophila melanogaster* does. Regarding the functions of these proteins, they can be simplified in four physiological areas: modulating the gene expression on development, differentiation, metabolic homeostasis and reproduction (Robinson-Rechavi *et al.* 2003).

The NRs modulate gene transcription throughout different mechanisms depending if there is, or not, the presence of a ligand. Endogenous ligands have not yet been discovered for all members of the superfamily. It is considered that we only know ligands for half of the NR superfamily members, the rest, those who are yet to be discovered a ligand that modulates their activity are known as orphan receptors.

Generally, ligands are lipophilic substances that can interact with NRs and induce a subsequent response that in most cases includes a target-gene DNA binding stage that modulates transcription, positively or negatively, by the interaction with coactivators or corepressors. Many genes regulated by NRs are identified as key responsible elements of various diseases. Therefore, it is reasonable to think that many drugs being developed nowadays are targeting them. Only in 2006, 13% of the approved drugs by the U.S. Food and Drug Administration (FDA) were targeting NRs. (Overington *et al.* 2006).

The NR localisation within the cell can be heterogeneous depending on the receptor. Whereas some can be constitutively localised inside the nucleus such as Peroxisome Proliferator-Activated Receptor (PPAR) or Retinoid X Receptor (RXR), others in exchange can be found in the cytoplasm of the cell under basal conditions but can translocate to the nucleus when

binding to their respective ligands as happens with the Glucocorticoid Receptor (GR) and glucocorticoids (GC).

As for the NR superfamily classification, initially was based on ligands, DNA binding properties and other functional characteristics (Vanden Heuvel 2009). Later in time, after the Human Genome Project, this classification was remade and is now divided phylogenetically, according to their amino acid sequence similarities, into 6 major subfamilies (NR1-6).

1.1 Nuclear Receptor Structure

In terms of protein structure, NRs are highly similar among them. As shown in Figure I1, there is the N-terminal domain (NTD), where transcriptional regulation region activation function (AF)1 is located. This can transcriptionally modulate some genes, independently of ligand, when the receptor binds to a specific DNA sequence. In this region, there are many phosphorylation sites, which makes it the target of multiple kinases.

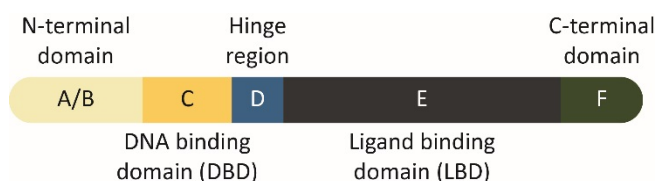


Figure I1. NR canonical structure. Based on what is described of NRs, five major regions can be identified. Beginning at the N-terminal end of the protein there is the N-terminal domain (NTD), comprising regions A and B, followed by the DNA binding domain (DBD) or region C, the most conserved region along within the family. This is divided from the ligand-binding domain (LBD), region E, by a less conserved hinge region (D) that gives the receptor some plasticity. The last, region F, corresponds to the C-terminal domain of the protein.

Next, there is the DNA-binding domain (DBD), the most conserved domain along the superfamily. This region not only binds to specific DNA sequences termed hormonal response elements (HREs) but it also contains a dimerization surface. Steroid receptors such as the GR bind almost exclusively as homodimers on HREs while others work as heterodimers with an obligate partner of the RXR group. As many NRs bind

to the DNA as a dimer, in most cases HREs are organized as two consensus hexanucleotide half sites arranged as direct, inverted or everted repeats and separated by a spacer of a variable number of nucleotides.

Between the DBD and ligand-binding domain (LBD) there is a less conserved region, the hinge region, that behaves as a flexible connector between the both domains and contains the ligand-dependent nuclear localization signal (NLS).

Finally, the C-terminal region contains the LBD, well conserved among NRs. LBD is made by 12 α -helices that fold to form the ligand binding pocket, and contains the ligand-dependent transactivation function, AF-2, whose activity depends on the integrity of the highly conserved amphipathic helix 12 located at the C-terminal end of the LBD. Binding of the ligand induces conformational changes in the LBD, resulting in movement of helix 12, which creates a new surface for the recruitment of coactivators that include the p160 family (SRC-1/ NCoA1; TIF2/GRIP-1/SRC-2; p/CIP/RAC3/ACTR/AIB-1/ TRAM-1) and p300/CBP. These coactivators, which have intrinsic acetyltransferase activity, recruit other large complexes with adenosine triphosphate (ATP)-dependent histone remodelling, histone acetyltransferase (PCAF), histone methyltransferase (CARM1/PRMT1) and histone kinase activities (Moras & Gronemeyer 1998; Rochette-Egly 2003).

1.2 Nuclear receptor transcriptional regulation

As reflected above, NRs are key elements in several transcriptional pathways. On this matter, different mechanisms of action have been described according to the outcome of its interaction with the DNA.

In the absence of ligand, many NRs repress gene transcription by recruiting corepressor proteins, such as the Nuclear receptor CoRepressor (NCoR) and the Silencing Mediator of Retinoic acid and Thyroid hormone

Introduction

receptors (SMRT). Corepressors are thought to function by antagonizing actions of coactivators and by recruiting factors that establish more repressive states of chromatin structure (Wagner *et al.* 2003).

On the other hand, ligand binding to the receptor induces a conformational change within the LBD that allows it to translocate into the nucleus where they can bind to DNA as homodimers, which is the case of the steroid receptors, or as heterodimers. In some occasions, this last case consists of an interaction with an obligate partner, the RXR. For those receptors which are constitutively located in the nucleus bound to DNA, interaction with the ligand induces a conformational change that modifies protein interaction properties. Subsequently, coregulatory and chromatin remodelling complexes are recruited to induce transcriptional modulation. As a final step, the transcriptional machinery (RNA polymerase II and its associated transcription factors) can be activated if there is to be an outcome of gene activation. Although there are fewer examples, gene transcriptional repression can also be mediated by this DNA binding-based mechanism through the recruitment of corepressors induced by the interaction of the NR with the ligand.

NRs can also lead to transcriptional repression in a DNA binding-independent manner such is the case of the GR on the activity of Activator Protein 1 (AP-1). In this particular example, the GR is believed to act as a monomer and by interacting with the AP-1 complex can negatively modulate the expression of AP-1-driven genes. This mode of action is termed *transrepression* as there is no direct binding of the NR to DNA but a protein-protein interaction throughout which the action is executed.

A very important aspect of NR regulation is through post-translational modification (PTM). PTMs are considered essential to cascade transduction as small protein modifications can underlie enormous

functional changes. PTMs can be divided in two groups: Reversible and Polypeptide Addition modifications. The former includes addition or removal of chemical groups such as phosphate, acetyl or methyl. The latter contains bigger modifications in terms of size such as SUMOylation, or ubiquitination (Anbalagan *et al.* 2012). One or more PTM or the same at different residues can occur on the same protein. Also, as part of a cascade, NRs can be target of subsequent PTMs the first being the triggering signal of the second. A clear example would be the phosphorylation-dependent ubiquitination of androgen receptor (AR), which results in degradation of the receptor by the proteasome (Lin *et al.* 2002). Further specific examples of this regulation will be matter of discussion in the following sections of this dissertation as are of highly interest in the research of how NRs crosstalk with different proteins.

1.3 Glucocorticoid receptor (GR)

GR and its ligands, GCs, are essential for life as shown in GR-deficient mice which dies shortly after birth due to severe abnormalities (Cole *et al.* 1995). Human GR (hGR) consists of two different isoforms, hGR α and hGR β , encoded by the *nr3c1* gene. They differ from each other in sequence and functionality. The length of the hGR isoforms is 777 and 742 amino acids, respectively, as a result of alternative splicing encoding the C-terminal region of the receptor (Smoak & Cidlowski 2004). hGR α is expressed in every cell type and carries out most, if not all, GC actions, including the anti-inflammatory responses. On the other hand, GR β does not bind hormone and may theoretically act as a dominant-negative inhibitor of GR α by interfering with its binding to DNA (Barnes 2011).

GCs are considered the most effective anti-inflammatory drugs available for the treatment of many chronic inflammatory and immune diseases (Barnes 2011). However, due to their pleiotropic actions, this therapy is

associated with the risk of side effects, especially at higher doses and long treatments (see Curtis *et al.* 2006; Hoes *et al.* 2009; Huscher *et al.* 2009).

Due to their lipophilic nature, GCs diffuse through the plasma membrane by a passive process and bind to the intracellular GR α , which is sequestered in the cytoplasm as a high affinity complex, consisting of heat shock proteins (hsp)90, hsp70, hsp56, hsp40, a low-molecular weight protein (p23), and several immunophilins (Smoak & Cidlowski 2004).

Upon binding to its ligand, GR α becomes activated, dissociates from the multimeric complex, thereby exposing its NLS that promotes rapid translocation to the nucleus. Once inside, it may increase the transcription of a vast array of genes including those for anti-inflammatory proteins including GILZ, lipocortin-1, interleukin(IL)-10, IL-1 receptor antagonist and neutral endopeptidase among others by binding to the GC response elements (GRE) located in their respective regulatory regions. It also can inhibit the expression of multiple inflammatory genes (transcriptional repression mechanism or transrepression) (Barnes 1998).

According to Clark (2007), GCs can exert its anti-inflammatory and side effects not specifically by transrepression and transactivation mechanisms, respectively, as it was thought in the beginning but by a more complex mode of action that, in addition to transactivation and transrepression, may also include post-transcriptional-dependent mechanisms.

1.4 Peroxisome proliferator-activated receptor (PPAR)

PPARs act as transcriptional modulators of genes related to glucose and lipid metabolism, immune response, adipogenesis and tumorigenesis. So far three subtypes of PPAR have been identified (PPAR α , PPAR β/δ and PPAR γ) encoded by three different genes (*nr1c1*; *nr1c2*; *nr1c3*, respectively). These, present a differential distribution within tissues and

therefore, perform different functions in different cell types. In humans, the alpha subtype has a major representation in the liver, kidney, muscle and heart; the beta is, in contrast, ubiquitously expressed and involved in the regulation of a variety of processes, while the gamma is expressed in adipocytes and macrophages (Youssef *et al.* 2013). In Table I1, a summary of the isoform tissue distribution, cell process involvement and physiological functions are shown (Desvergne & Wahli 1999).

	PPARα	PPARβ/δ	PPARγ
Tissue distribution	Liver, kidney, muscle, heart	Ubiquitously expressed	Adipose tissue, macrophages
Cellular process	Mitochondrial and peroxisomal β -oxidation	Mitochondrial β -oxidation, ROS reduction	Adipocyte maturation and triglyceride synthesis
Physiological function	Lipid metabolism, wound healing, control circadian rhythm	Lipid metabolism, liver regeneration	Adipogenesis, glucose homeostasis and inflammation

Table I1. PPAR main characteristics in mammals.

PPARs heterodimerize with RXR and bind to PPAR response elements (PPREs) which are composed by two direct (or inverted) repeats of the hexamer 5'-AGGTCA-3' spaced by a single nucleotide.

In some parts of this project we will be focusing the effects of PPAR γ specifically and therefore a few more insights are needed to completely understand its mechanisms and actions. From a clinic point of view, perhaps it is true that this subtype is the most studied one because of its implications in relevant diseases such as type 2 diabetes (T2D) or cancer

Introduction

(Rosen & Spiegelman 2001). PPAR γ exists in two protein isoforms: PPAR γ_1 and PPAR γ_2 . The origin for such variation relies in alternative promoter usage and splicing at the 5' end. PPAR γ_2 contains 30 extra amino acids at the N-terminal end of the protein compared to PPAR γ_1 . Additionally, PPAR γ_2 is adipose tissue-specific so its expression levels in this tissue are very high. On the other hand, PPAR γ_1 has an ubiquitous low expression in many tissues that include heart, skeletal muscle, pancreas, intestine and adipose tissue.

Regarding the natural ligands for these receptors there is no specific ligand for each isoform but a group of fatty acids and more specifically, certain eicosanoids, derived from polyunsaturated fatty acids (PUFAs) have been shown to bind PPAR γ with high affinity and activate it (Reginato *et al.* 1998; Yu *et al.* 1995). Also, it is known that the differential distribution of endogenous ligands through different tissues can trigger specific outcomes. Therefore, due to diet-related ligand availability, activation of PPAR γ can be limited to precise tissues and resulting in a more specific activation (Grygiel-Górniak 2014).

Synthetic ligands for this NR have also been generated. The most potent are thiazolidinediones (TZDs) (Lehmann *et al.* 1995) and FMOC-L-Leucine (F-L-Leu) (Rocchi *et al.* 2001). Among the TZDs, which will be focused on this project, rosiglitazone, troglitazone and pioglitazone are considered useful for the treatment of T2D due to their insulin sensitizing actions (Nolan *et al.* 1994). The commercialisation as antidiabetic drugs began in the 90's. However, due to liver toxicity and cardiovascular related side effects they were slowly withdrawn from the market.

As previously mentioned, two major roles of PPAR γ are related to anti-inflammatory processes and adipogenesis. Regarding the anti-inflammatory effects mediated by this NR, they are exerted throughout

mechanisms of transrepression and may require PTMs of the receptor (Brunmeir & Xu 2018). Examples of such behaviour can be found in the modulation of several cytokines such as tumour necrosis factor- α (TNF α), interferon- γ (IFN γ), IL-1 β , IL-6 or transcriptional factors such as nuclear factor kappa-light-chain-enhancer of activated B cells (NF- κ B) or AP-1 (Ricote & Glass 2007). On the other hand, regarding adipogenesis, it is known that PPAR γ binds the enhancers of crucial adipogenic genes such as *aP2/fabp4* or *pck1* (coding for fatty acid-binding protein 4 (FABP4) and phosphoenolpyruvate carboxykinase (PEPCK), respectively) increasing its gene expression (Tontonoz *et al.* 1995). Also, during adipocyte maturation the accumulation of lipids is linked to the increase expression of genes involved in lipid metabolism that have also been identified as PPAR γ target genes (Siersbæk *et al.* 2010). Different *in vivo* studies have been performed in this direction with PPAR γ knockout mice. Animals lacking PPAR γ were unable to survive due to severe problems at the embryonic development. Also, PPAR γ -deficient fibroblasts presented diminished adipogenic maturation *in vitro* (Barak *et al.* 1999; Kubota *et al.* 1999).

1.5 Liver X Receptor (LXR)

Liver X Receptors (LXRs) behave themselves as regulators of the lipid and glucose metabolism as well as proliferation and inflammation modulators. Two different isoforms have been described, LXR α and LXR β , encoded by separate genes, *nr1h3* and *nr1h2*, respectively. As happened with PPAR γ , there is one isoform that is distributed ubiquitously, the beta isoform, while the alpha isoform is found to be restricted to macrophages, white adipose tissue (WAT), liver, intestine, kidney and spleen (Pascual-García & Villedor 2012).

In order to modulate gene expression LXRs, as PPARs, must form an heterodimer with its obligate partner RXR with whom bind to LXR

Introduction

response elements (LXREs) located in promoters or enhancers of target genes and composed by two direct repeats separated by four random nucleotides as follows: 5'-DGKTYANNNNHGKKCA-3'* (Edwards *et al.* 2002). Synthetic agonists for this receptor have also been developed during the years. A clear example is the GW3965 or T0901317, which are agonists able to modulate LXR target pathways (Pascual-García & Valledor 2012).

Physiologically, LXRs are considered essential metabolic regulators. At the beginning they were discovered as mediators of cholesterol homeostasis. Several natural oxidized forms of cholesterol (oxysterols) have been identified to activate these receptors. When systemic cholesterol is accumulated the level of oxysterols increases too, meaning that body sensors are activated to decrease the excess of sterols. For that task, sterol transporters such as ABCA1 and ABCG1, downstream of LXR cascade, direct the cholesterol efflux to the high-density lipoproteins (HDL) so it can be transported to the liver and secreted as bile salts and faeces and therefore limiting its intestine absorption (Peet *et al.* 1998; Repa *et al.* 2000).

LXR also plays a crucial role in glucose metabolism in the adipose tissue inducing the migration of glucose transporter 4 (GLUT4) vesicles to cell membrane in order to increase glucose uptake in response to insulin or inhibiting gluconeogenic genes such as PPAR γ coactivator-1 α (PGC-1 α) or PECK in the liver (Laffitte *et al.* 2003). Furthermore, LXR promotes lipogenesis through the expression of sterol regulatory element-binding protein 1c (SREBP1c) and carbohydrate response element-binding protein

* IUPAC nucleotide code

A: Adenine, T: Thymine, G: Guanine, C: Cytosine, D: A or G or T, K: G or T, Y: C or T, H: A or C or T, N: any nucleotide.

(ChREBP), both controlling biosynthesis of fatty acids (Pascual-García & Valledor 2012) and, in the case of the former, of cholesterol, too.

On another level, LXR takes part in the anti-inflammatory response cascade. It is known that when synthetic agonists of LXR are used against lipopolysaccharide (LPS), IL-1 β , TNF α or IFN γ pre-activated pathways, these are repressed. Nonetheless, it is also known the effect of LXR agonists also depends on the cell type and the inflammatory stimuli meaning that not all agonists may repress the same inflammatory pathways under similar conditions in all cell types.

1.6 Retinoid X Receptor (RXR)

The last NR introduced is the Retinoid X Receptor (RXR), which in this project will only be mentioned as an obligate partner for PPAR γ and LXR. Nonetheless, RXR has three isoforms (alpha, beta and gamma) encoded by three genes *nr2b1*, *nr2b2* and *nr2b3*, respectively. RXR γ is mainly expressed in brown adipose tissue (BAT) and RXR α in WAT (Villarroya *et al.* 1999). A natural ligand for this receptor is 9-cis-retinoic acid, a derivate of vitamin A (Ziouzenkova & Plutzky 2008). On the other hand, synthetic agonists have also been developed such as LG268.

2. Mitogen Activated Protein Kinases (MAPK)

Another important part of this project belongs to the mitogen-activated protein kinases (MAPKs), which are proline-directed serine-threonine protein kinases involved in signal transduction. In mammals, there are more than a dozen MAPK enzymes that regulate cell proliferation, differentiation, motility, inflammation and survival (Cargnello & Roux 2011). As it happens with NRs, MAPKs are highly conserved throughout evolution in eukaryotes (Kyriakis & Avruch 2001).

Authors consider MAPKs subdivided in conventional and atypical according to their activation mechanism. Conventional MAPKs include extracellular signal-regulated kinases (ERK)1/2, c-Jun N-terminal kinase (JNK)1/2/3, p38 α , β , γ , δ , and ERK5. Although sharing similar sequences ERK3/4/7/8 and Nemo-like kinases are not included in the group above due to its different activation mechanism and are considered, according to Cargnello & Roux (2011), *atypical* MAPKs. In the end, the most extensively studied by far are the first three groups within conventional MAPKs.

Activation of MAPKs depends on phosphorylation of threonine and tyrosine residues within a conserved motif Thr-X-Tyr, located in the activation loop, where X represents a specific amino acid depending on the MAPK (Kyriakis & Avruch 2012). For example, JNK motif consists on a proline in the X position while ERK has a glutamate and p38 has a glycine (Ahn *et al.* 1992; Kyriakis *et al.* 1994; Lee *et al.* 1994).

2.1 MAPK Regulatory Mechanisms

Each of these so-called conventional MAPKs is the final step of a three-tiered kinase cascade (MAPK module), which is composed of a set of three independent sequentially acting kinases: a MAPK, a MAPK kinase (MAPKK or MAP2K) and a MAPKK kinase (MAPKKK or MAP3K) (Figure I2). The signal transduction begins with an extracellular stimulus such as mitogens, cytokines, growth or stress factors that trigger the cascade where several phosphorylation events take place. Small GTP-binding protein of the Ras/Rho family are often involved in the process at very early stages of the cascade (Cargnello & Roux 2011). Briefly, MAP3K leads to phosphorylation and activation of a MAP2K, which in turn activates the MAPK through dual phosphorylation on Thr and Tyr residues. The end of this three-step event of the MAPK cascade is the activation of the MAPK-activated protein kinases (MAPKAPK) which contains members of the p90

ribosomal S6 kinases (RSK), mitogen- and stress-activated kinases (MSK), MAPK-interacting kinases (MNK) and MAPK-activated protein kinases (MK), among other substrates some of which are transcriptional regulators (Cargnello & Roux 2011).

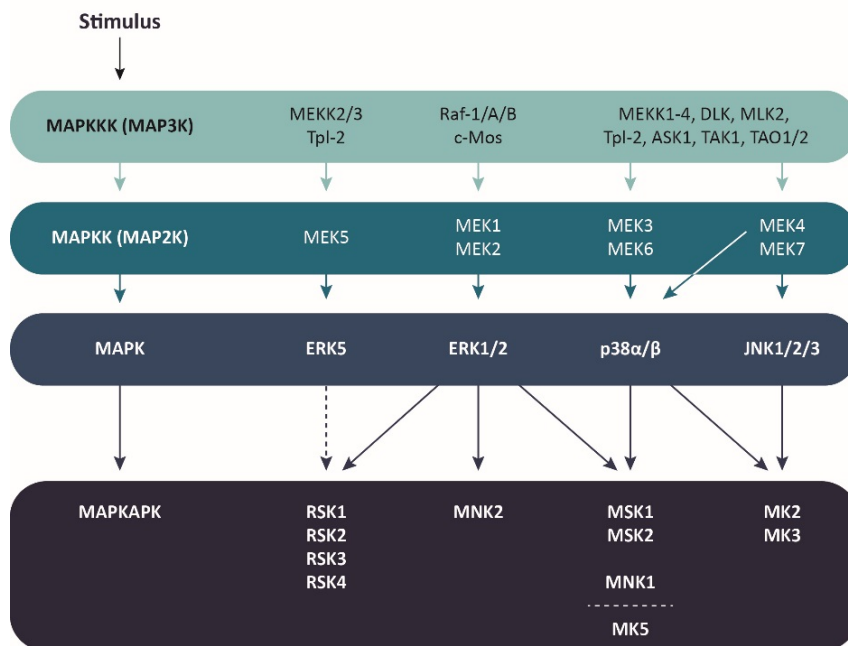


Figure 12. MAPK signal transduction from initial stimulus to MAPKAPK (Adapted from Cargnello & Roux 2011). The diagram shows how from specific stimuli the signal cascade can activate specific target-proteins. Dotted lines indicate that substrate regulation remains to be *thoroughly* demonstrated.

These steps are meant to amplify the signal where not only one target is activated but several outputs are accomplished through differential magnitude or extent of the MAPK activation. On the other hand, less is known about the *atypical* MAPK pathway activation. It is known that these proteins are not organised into three-tiered kinase cascade and they do not share the Thr-X-Tyr motif. Only in the case of ERK7 this motif and phospho-sites are conserved, but the absence of a distinct upstream

MAP2K makes ERK7 undergo activation through auto-phosphorylation (Cargnello & Roux 2011). MAPK activity is also subjected to negative regulation by dephosphorylation by MAPK phosphatases/dual specificity phosphatases (MKPs/DUSPs). These phosphatases can act on both Thr and Tyr phospho-site residues of activated MAPKs (Caunt & Keyse 2013).

2.2 Stress Activated Protein Kinases (SAPK)

Within MAPKs, JNK and p38 subfamilies are activated by cellular stressors. Therefore, altogether they are considered Stress Activated Protein Kinases (SAPK). On the one hand, JNK (or p54 in older references) was initially identified as a cycloheximide-response MAPK in rats (Kyriakis & Avruch 1990). Later it was also linked to c-Jun phosphorylation on Ser63/73 and further research also identified several JNK roles in response to heat shock, ionizing radiations, cellular stress, genotoxins, cytokines and protein and DNA synthesis inhibitors (Barr & Bogoyevitch 2001). JNK are encoded by three different genes, *jnk1*, *jnk2* and *jnk3*, that due to alternative splicing lead up to ten different isoforms that differ in size between 46 and 55kDa and share an amino acid sequence similarity of 80 to 85%. When it was first discovered it was thought that this similarity would give very similar tissue distribution and function, but the truth is that it was not. While *jnk1* and *jnk2* seem to have a broad tissue distribution, *jnk3* is primarily found in neuronal tissue and to a lesser extent in testis and heart (Bode & Dong 2007). Besides, knockouts of each gene confirmed different functions. As an example, *jnk3*-deficient mice showed apoptosis-resistance in neuronal cells implicating JNK3 in the regulation of programmed cell death in this cell type. Single *jnk1*- or *jnk2*-deficient mice revealed functional redundancy and overlapping expression while the double *jnk1/2*-deficient mice die early at embryogenesis (Dong *et al.* 2002). Single deficient mice revealed also resistance to several pathologies including obesity, T2D,

arthritis, hepatic issues or heart cell death in the *jnk1*-deficient and type 1 diabetes, arthritis, tumoral growth, atherosclerosis or heart cell death in *jnk2*-deficient mice (Bogoyevitch 2006). Thus, in line with diverse studies reflecting the functional importance of JNK isoforms, the use of isoform specific JNK modulators can become an important therapeutically tool to improve some of the mentioned diseases.

Regarding p38, the first isoform described, p38 α , was the result of an endotoxin and osmotic shock response test where a 38kDa peptide homologous to Hog1p, a MAPK from *S. cerevisiae* activated by hyperosmolarity, was purified (Kyriakis & Avruch 2001). From the four gene-independent isoforms mentioned before, alpha is expressed at high levels in most tissues while the beta, gamma and delta have some sort of specificity in brain, skeletal muscle and endocrine glands, respectively. However, when one isoform is compromised, it has been demonstrated certain redundancy which will correspond to increased expression of an alternative viable isoform. p38 α and p38 β or p38 γ and p38 δ pseudo-groups revealed independent phosphorylation substrates (Cuadrado & Nebreda 2010).

Canonical activation mechanisms involving both MAP3K and MAP2K are shown in Figure I2. Roughly, JNK motif Tyr-Pro-Thr is phosphorylated by MKK4/SEK1 and MKK7/SEK2. The latter is specific for JNK while the former can also activate other MAPK (see below). In turn, these are activated by phosphorylation events at Ser/Thr residues within a Ser-Xaa-Ala-Lys-Thr motifs by several MAP3Ks including MEKK1–4, the protein kinases of the mixed lineage kinase (MLK) family, apoptosis signal-regulated kinase (ASK)1, and TGF β -activated kinase (TAK)1 (Widmann *et al.* 1999).

To the same extent, the four p38 isoforms can be phosphorylated at Tyr-Gly-Thr motif by MKK6 but only alpha, gamma and delta by MKK3.

Additionally, MKK4 has also been observed to activate p38 α (Doza *et al.* 1995). The relative contribution of MAP2K to p38 activation always depends on the cell type and stimulus applied. These are also activated by phosphorylation events in Ser/Thr residues within a Ser-Xaa-Ala-Xaa-Thr motif by various MAP3K, many shared with the JNK cascade, including MEKK1-3, MLK2/3, ASK1, tumor progression locus (Tpl)2, TAK1 and thousand and one-amino acid kinase (TAO)1/2.

3. c-Jun N-terminal Kinase (JNK) – Nuclear Receptor Interaction

For several years Dr. Caelles laboratory has focused on the important role of the crosstalk of NRs and SAPK. Particularly, the inflammation-related interaction of JNK with different NRs. On this project we have focused our efforts to resolve some insights of these interactions within some NRs.

3.1 JNK – GR

As commented on a previous section, GC anti-inflammation actions and, in general, the inhibition of immune cell activation, represented a good pharmacological perspective and GCs were distributed as medical hormones to treat various pathological conditions such as asthma, allergic rhinitis, rheumatoid arthritis and leukaemia (Barnes 1998). The main actions of GCs rely on binding to intracellular GR triggering a morphological conformation and translocating the complex to the nucleus where it can dimerize, bind to GREs and exert its DNA-modulation actions inducing anti-inflammatory genes or regulating the expression of other inflammatory pathways.

Dimerization studies have shown that despite the importance of this mechanism, it is not essential. Mice harboring a GR dimerization mutant (GR^{dim}) survive to adulthood, unlike GR-deficient mutant mice (Reichardt *et al.* 1998). The study mentioned, manifested that the set of genes

modulated by GR^{dim} in response to ligand are those under the positive control of AP-1 and NF- κ B. Therefore, an initial conclusion obtained was that anti-inflammatory actions through which GR controls downstream effectors of pro-inflammatory pathways were mediated by the transrepression function of GR. However, more recent studies on this subject supported that the initial assumptions concluding that GR^{dim} was unable to create GR dimers were premature (Nixon *et al.* 2013). Frijters *et al.* (2010) described that in this mice GR^{dim} was able to induce, to a lower extent than in WT littermates, GR-dependent transactivation in response to GCs. Later, Jewell *et al.* (2012) shed new light on this matter with the possibility that alternate homodimer formation could be responsible for such events. This opened the possibility to consider that GR could have multiple contact regions within the same monomer. An idea inferred from the AR, where contacts between the LBD and the NTD within a single molecule can happen upon activation (Nixon *et al.* 2013).

The antagonism between GR and the transcriptional factor AP-1 was described in early 90s and some studies suggested that GR repression occurred with promoter-bound AP-1 preventing it to activate transcriptional machinery. Later on, others suggested that the interference was upstream, at the level of MAPK (Caelles *et al.* 1997). In this regard, on 2003 Bruna *et al.* described the mechanism by which, upon ligand administration, GR can mediate a direct docking interaction with JNK and dissociate it from MKK7-JNK complexes. Then, the GR-JNK complex translocates to the nucleus where through JNK-AP-1 binding repress the induction of AP-1 target genes (Figure I3). They also observed that the interaction between JNK and GR was not found in any other member of the NR superfamily. Even so, GR amino acid sequence analysis of the JNK docking site also revealed that it was preserved during evolution

Introduction

seeing that different species maintained the same amino acid sequence. Later, other transcription mediated mechanisms, such as GC-dependent induction of MKP-1/DUSP-1 were reported to also mediate the GR interference on JNK activation (Kassel *et al.* 2001).

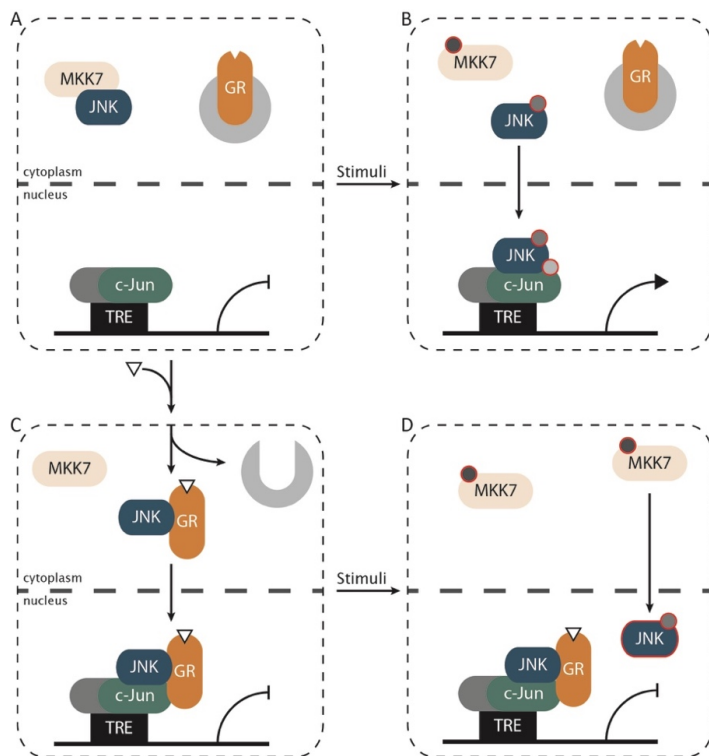


Figure 13. GC effect on JNK activation mechanism (Adapted from Bruna *et al.* 2003). (A) In the absence of its ligand, GR remains in the cytoplasm associated to accessory proteins such as chaperones. In the same stage, JNK is maintained at the same cell compartment associated to MKK7 by scaffold proteins. AP-1 protein containing c-Jun is bound to TPA response elements (TRE) while the AP-1 target gene remains inactive. (B) When the cell is stimulated, several phosphorylation (grey circles with red outlines) events transduce the signal that finally activates the transcription of the AP-1 target gene. First steps include phosphorylated/activated JNK dissociation from MKK7 complex and entering to the nucleus where it binds to, and phosphorylates, AP-1, thereby releasing the corepressor complex, allowing interaction with co-activators and, eventually, transcriptional activation. (C) Upon entering the cell, GC (inverted white triangle) binds to GR, which by exposing the JNK docking site, binds to JNK and translocate together to the nucleus. There, the GR-JNK complex associate to c-Jun but as JNK is inactive, fails to phosphorylate/activate it. Therefore, the transcription activation is not accomplished. (D) In this scenario, the cell stimulus fails to activate the AP-1 target gene. It is worth mentioning Even more, the GR-JNK complex prevents the interaction of active JNK with its substrate c-Jun.

On the other hand, it has also been observed that the sequence of events demonstrated above are time sensitive meaning that is very important which stimulus comes in first and/or stays longer. In the example mentioned in Figure 13 GCs were first administered but if, on the opposite, the JNK stimulus comes in first or stays for longer time a completely different outcome may be obtained. On these cases there has been reported an increased GR-nuclear export due to increasing levels of phosphorylation on hGR Ser226 (Itoh *et al.* 2002; Wang *et al.* 2007) resulting in less activation of GR target genes and partially restored when mutants of this region were investigated (Rogatsky *et al.* 1998). This alternate output might account for a decreased response to GCs, a relevant clinical situation generally known as GC resistance whose responsible mechanisms are an intense focus of study (Barnes 2010)

3.2 JNK – PPAR γ

The second crosstalk involved in the negative regulation of JNK includes PPARs. Our focus on this NR subfamily will be specifically on PPAR γ . TZDs are PPAR γ synthetic ligands that have significant pharmacological results as insulin-sensitizing agents. This insulin-sensitizing action relies on the inhibition of JNK activation by TZD activated PPAR γ (Díaz-Delfín *et al.* 2007). Under normal conditions JNK does not interfere in the correct insulin signalling cascade. Briefly, in normoglycemia states glucose transporters GLUT1/3 maintain passive glucose uptake as a source of energy. In hyperglycaemia, due to the inability of these transporters to assimilate the excess of glucose, GLUT2 transporters, which are mainly expressed in pancreatic β -cells, liver and kidney are responsible of internalise glucose in those cells (Navale & Paranjape 2016). In this condition, in pancreatic β -cells, glucose is metabolised through glycolysis increasing the ATP/ADP ratio. Consequently, the K⁺ channels are closed,

Introduction

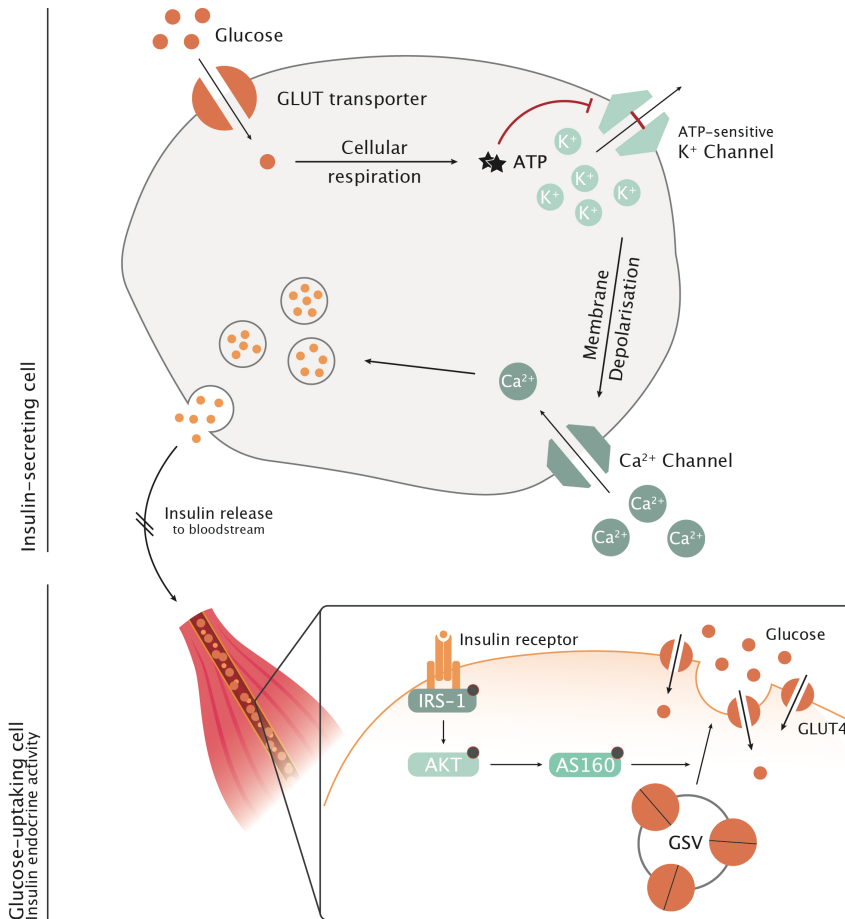


Figure 14. Glucose to insulin cascade activation. Top panel shows the effect of increased glucose level on insulin-secreting cells. Bottom panel displays the endocrine effect of insulin within a glucose-up taking cell such as muscle cells. Three basic steps in the insulin signalling cascade are represented: phosphorylation of IRS-1, AKT and AS160 which lead to the externalisation of GLUT4 to the cell membrane.

and the cell membrane potential is depolarized. As a result, the Ca^{2+} channels open and insulin is released to bloodstream.

In a paracrine manner, insulin also induces a positive feedback on surrounding pancreatic β -cells increasing insulin release. In an endocrine manner, on peripheral tissues, insulin binds to its receptor and induces recruitment and phosphorylation of IRS-1 on Tyr residues. After several

phosphorylation events of downstream mediators ends with the fusing of GLUT4 storage vesicles (GSV) to cellular membrane exposing stored GLUT4 to the extracellular space giving the cell the ability to internalise glucose (Figure 14). In both cellular scenarios, the insulin cascade can be interrupted by JNK at initial stages with a phosphorylation of IRS-1 at a particular serine residue (Ser-307 in human IRS-1), which dissociates it from the InsR and thereby, blocks the signal transduction to downstream effectors. (Aguirre *et al.* 2000). On 2007 Díaz-Delfín *et al.* showed that the administration of the TZD rosiglitazone inhibited the TNF α -induced phosphorylation/activation of JNK but not the overall JNK amount. In this context, they described that in *ob/ob* mice after TZD administration the Tyr phosphorylation on IRS-1 was significantly increased. Moreover, the *in vivo* insulin-sensitizing action of rosiglitazone was abolished in obese JNK-1 knockout mice, indicating that JNK inhibition is required for TZD to perform this important pharmacological action. Moreover, *in vitro* PPAR γ knockdown or the use of PPAR γ antagonists ablated JNK inhibition by TZDs. Consistently, when the amount of PPAR γ was increased by overexpression the TZD inhibitory effect on JNK activation was exacerbated. Overall, these observations indicate that TZD inhibitory action on JNK activation is mediated by PPAR γ . More in-depth specifics of this disease-related mechanistic will be developed further in this section.

4. JNK-NR crosstalk: from targeting inflammation to drug resistance

Inflammation is considered an adaptive response to internal or external perturbations that exceed homeostatic capacity of the system. Understanding the molecular and cellular mechanism involved in this process is still in progress. Truly, acute inflammation events related to infection or tissue injury are considerably well known. On the other hand,

localised chronic inflammation and autoimmune diseases are partially understood but less is known about causes and mechanisms of systemic chronic inflammation, which takes part in a wide variety of diseases (Figure 15).

This last *state* does not seem to be caused by usual agents such as infections or injuries but a tissue malfunction instead, which creates a homeostatic imbalance that is not directly related to host defence or tissue repair mechanisms (Medzhitov 2008). Given the fact that overcoming the inflammatory stimuli is important it is not surprising that it is subjected to coregulation at multiple levels.

4.1 GC therapeutic response

GCs are released under stress situations. They are used in the treatment of inflammatory diseases such as psoriasis, rheumatoid arthritis, eczema, chronic obstructive pulmonary disease or asthma, among others. It is known that they antagonize the transcriptional actions of several pro-inflammatory mediators, key to amplify the inflammatory responses such as NF- κ B and AP-1 (Smoak & Cidlowski 2004).

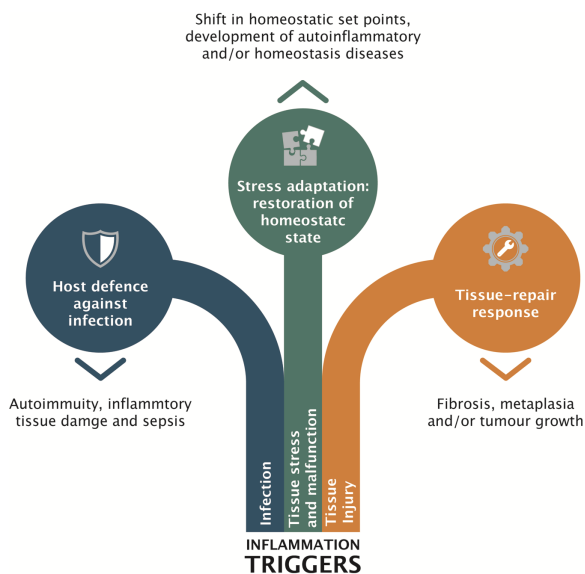


Figure 15. Inflammation causes and pathological outcomes (adapted from Medzhitov 2008). Depending on each trigger, the inflammatory response leads to different pathological outcomes. From these, only the infection-induced inflammation is linked with the activation of an immune response.

On this context, they have been shown to have a powerful impact on the disease improvement. Nonetheless, apart from its well-known secondary effects during long-term treatments, resistance to treatments have already been observed. Peter J. Barnes reviewed and investigated several mechanisms related to clinical impairment of GC action summarised in Figure 16 (Barnes 2010). Interestingly, not only GCs can control inflammation processes but vice versa. A clear example is found when hGR is phosphorylated at Ser226 or there is an excessive activation of AP-1. It is known that in both cases the interaction GR-GREs is altered resulting in a decreased activation of GR target genes. Additionally, it is described that phosphorylation of hGR Ser226, mainly carried out by JNK upon activation, induces localisation changes of the receptor within the cell. It is believed that due to this PTM, GR is exported to the cytosol blocking its ability of inhibiting pro-inflammatory and activating anti-inflammatory genes (Itoh *et al.* 2002; Rogatsky *et al.* 1998). Moreover, MKP-1 is also observed to be upregulated by GR (Kassel *et al.* 2001).

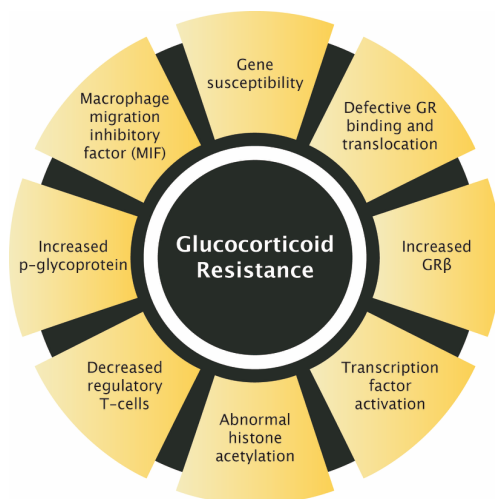


Figure 16. GC resistance molecular mechanisms. The lack of responsiveness to GC usually leads to an increase of dose which also increases the risk of side effects that this treatment might cause. Although risk is high and benefits are rarely significant treatment resistance can be acquired, not just related to GC dose-related, and can be attributed to at least one of these groups.

On this context, the mutual negative control between GR and JNK can play a double-edge role depending on the strength in which each pathway is activated. For example, in a situation where GR is active, JNK activation can be modulated normally and anti-inflammatory effects of the receptor can be triggered correctly, mainly through MKP-1. On the other hand, under a GC resistance condition where JNK activation is exacerbated, the ability of GR modulating JNK activation is much harder because the cell does not have any tool to apply enough negative pressure on the pro-inflammatory cascade already in motion.

Recently, Xia *et al.* (2019) reported that rosiglitazone combined with GCs can improve GC resistance in guinea pigs suffering from sensorineural hearing loss through enhanced expression of MKP-1, which is decreased in GC resistant patients (Moosavi *et al.* 2017), and lead to inhibition of p38 and NF- κ B activation.

4.2 Obesity, Type 2 Diabetes and Inflammation

In contrast to GCs, which are capable of inhibiting acute and chronic inflammation responses, PPAR agonists are relatively ineffective in acute settings. Instead, their effects are closely linked to metabolic abnormalities such atherosclerosis or obesity-induced insulin resistance (IR) (Glass & Ogawa 2006).

Obesity and T2D are two strongly associated metabolic diseases with higher prevalence index in developed countries. Unfortunately, the incidence rate of both diseases is rising quickly, and new therapeutic fronts are required in order to reduce both incidence and prevalence.

Clinically, T2D results from progressive pancreatic β -cell dysfunction caused by chronic IR, which is a defective response to insulin in peripheral tissues such as liver, adipose tissue and skeletal muscle. Molecularly, the mechanisms responsible for developing IR are yet to be fully characterized,

even though, there is clear proof that JNK pathway plays an important inhibitory role on early steps of the insulin receptor (InsR) signal transduction pathway. As summarised previously, JNK phosphorylates human IRS-1 on Ser307 and, inhibits IRS-1 tyrosine-phosphorylation by hormone-activated InsR (Aguirre *et al.* 2000; Ozcan 2004). Additionally, it is well established that JNK is activated by diverse stimuli found in the obese condition, such as endoplasmic reticulum stress (ERS), pro-inflammatory cytokines and reactive oxygen species (ROS).

Together with other pathways, prolonged JNK upregulation leads to a low-grade chronic inflammatory response originated in the adipose tissue and which is known as metabolic inflammation or *metaflammation* (Hotamisligil 2017) (Figure 17).

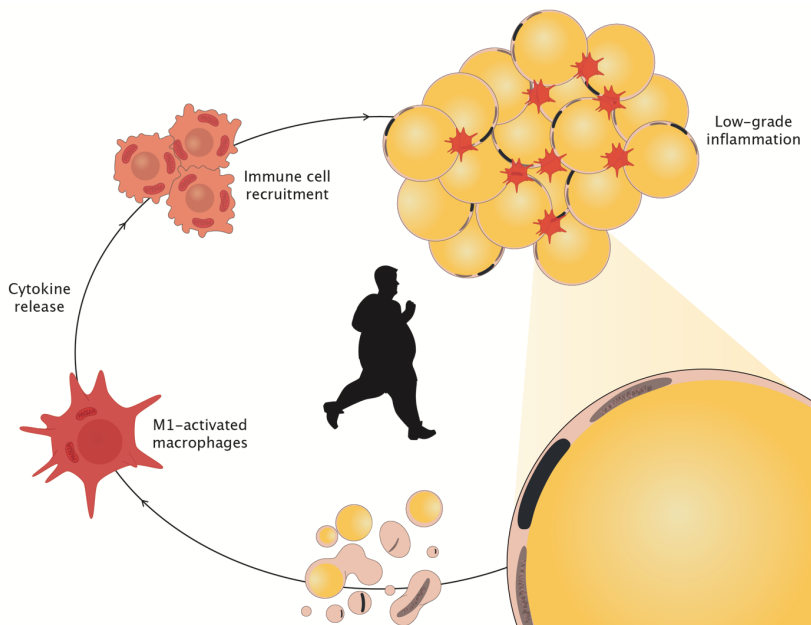


Figure 17. Early steps of *metaflammation*. The adipose cells in obese individuals are both greater in number and size than in lean individuals. As a result of sorting excessive amounts of fat, the stressed adipose cells release inflammation-inducing factors and undergo apoptosis. Both outcomes activate macrophages in a traditional M1 inflammatory state in which they release a $\text{TNF}\alpha$, which recruits and activates additional immune cells to the site. This low-level sustained inflammation causes tissues to become resistant to insulin, the first step in developing diabetes.

Introduction

In obesity, adipose tissue overexpansion leads to a hypoxic environment which in early stages of the disease begins to affect the homeostasis of the overall cellular population in the adipose tissue and, in particular, the adipocytes. Concretely, in the ER, the cellular organelle where proteins with specific subcellular fates are synthesized, folded into their correct three-dimensional structures, modified, and transported to their final cellular destinations, hypoxia conditions interfere with the creation of disulphide bounds in the lumen, resulting in ERS (Khan & Wang 2014). As a result of this condition the unfolded protein response (UPR) is triggered, which activates the three major pathways arising from the ER membranes: IRE1 α , PERK and ATF6 cascades. UPR attempts to cope the accumulation of unfolded proteins by inducing the expression of genes encoding chaperones and inhibiting the general protein synthesis but if this fails, UPR is also capable to induce cell death. On this line, the IRE1 α arm of the UPR leads to the activation of JNK, which is associated to the induction of the inflammatory response and the development of IR (Ozcan 2004). According to our data, PPAR γ , and also LXR, inhibit the activation of the JNK pathway several hours after the addition of the agonist ligand, therefore, it is likely that the inhibitory mechanism requires gene transcription (Díaz-Delfín *et al.* 2007). Therefore, we focused our attention on the identification of PPAR γ and or LXR target genes able to mediate in inhibitory action of these NRs on the JNK pathway

Keeping this in mind, we became interested in a PPAR γ -direct target gene, the insulin-induced gene (INSIG)-1, which can exert an adaptive response that preserves lipid homeostasis in obese and IR states (Kast-Woelbern *et al.* 2004). INSIG-1 is a transmembrane protein located in the ER membrane that functions as a modulator of cholesterol biosynthesis through its interaction with SREBP cleavage-activating protein (SCAP) (Feramisco *et*

et al. 2004), and has been linked to the action of PPAR γ since it is upregulated in response to rosiglitazone *in vivo*, in WAT and in C3H10T1 cells. Particularly, it has been observed that INSIG-1 gene promoter has two PPREs, which indicates the direct interaction between PPAR γ and INSIG-1 gene promoter (Kast-Woelbern *et al.* 2004).

The evidence presented lead us to the hypothesis of an interaction between the first steps of the ERS mechanism, which take place in the ER membrane, and INSIG-1, which is also located on the same membrane with a well-known ability of interacting to other transmembrane protein such as SCAP. Thus, if INSIG-1 could interact with the IRE1 α arm of ERS, it may be able to modulate IRE1 α -dependent activation of JNK and therefore the downstream pro-inflammatory cascade leading the IR state. Supporting our hypothesis are the observations by Chen *et al.* (2011) showing that INSIG-1 inhibits ERS-induced and JNK-dependent death of pancreatic β -cells.

We also directed our attention to the serine-threonine phosphatase, PP5, which was previously shown to negatively regulate MAPK through ASK1 *in vitro* and increased its levels under hypoxia and oxidative stress environments (Morita *et al.* 2001). *In vivo* experiments reported that PP5 gene transcription in specific tissues is induced by LXR ligands and requires LXR expression (Steffensen *et al.* 2004). Moreover, previous studies from the group showed that PP5 was responsible to inhibit LPS-induced activation of SAPK. This study confirmed the inhibitory effect of the LXR agonist T0901317 on LPS-activated SAPKs (JNK and p38), as well as observing that LXR ligand increases PP5 both at mRNA and protein level. Transient transfection experiments in HEK293T cells also revealed PP5-dependent ASK1, AP-1 and c-Jun modulation. In addition, SAPK inhibition by LXR agonist required LXR function and this action it is achieved after 6h

Introduction

treatment with LXR agonist on bone marrow derived macrophages (Çavusoglu 2013).

PP5 deficient mice have been studied in the context of obesity. Nevertheless, two different studies revealed controversial results. On the one hand Grankvist *et al.* 2013 published that PP5 knockout mice, achieved by deleting the first exon of the murine *ppp5c* gene, fed a 60%-fat diet from week 8 of age during 10 weeks were significantly leaner and preserved insulin sensitivity in comparison to wild-type mice fed with the same diet. Furthermore, glucose tolerance test (GTT) performed on animals on control diet indicated that glucose uptake was increased in PP5 knockout mice evidencing an alteration in pancreatic β -cells insulin secretion as described previously by the same group (Grankvist *et al.* 2012). On the other hand, Jacob *et al.* (2015) described a PP5-knock in mice achieved by a PP5 gene mutation that changes Asp274 to Ala rendering an inactive phosphatase. Under standard diet these mice showed significant lower weight differences compared to control animals. These significant differences between genotypes disappeared when animals were fed with 45%-fat diet from week 8 of age for 26 consecutive weeks. Interestingly, under this last condition a lower weight tendency could be observed for PP5-knock in mice although significance was only achieved in five out of the twenty-five weeks of diet. It should be noted that this tendency was visible from the sixth week of diet, when animals were already 14-weeks old. Regarding glucose homeostasis, GTT on 45%-fat diet animals at week 29-33 of age demonstrated a slower recovery to glucose basal levels for PP5-knock in mice. Insulin tolerance test was performed only on animals on standard diet showing a higher insulin sensitivity in PP5- knock in mice.

PP5 is also relevant for the GR function by targeting and dephosphorylating specifically phospho-Ser203 and phospho-Ser226 residues of hGR. Briefly, PP5 has been described as a component in the GR-Hsp90 complexes interacting directly with Hsp90 (Chen *et al.* 2008). On the above-mentioned paper (Jacob *et al.* 2015), it was also reported that PP5-knock in mouse embryonic fibroblasts (MEFs) acquire higher levels (10-fold) of phosphorylated GR at orthologous Ser211 and Ser203 sites compared to wild-type counterparts. When the effect of GR agonist dexamethasone on phosphorylation events was analysed, an 18-fold increase in wild-type MEFs while “marginal” increase in PP5-knock in was observed. However, this is not in agreement with Hinds *et al.* (2011) where they do not observe any basal receptor hyperphosphorylation and dexamethasone induction reports similar phosphorylation levels between genotypes.

Finally, it is important mentioning the existing three-edge crosstalk between GR, PPAR γ and PP5 on lipolysis and lipogenesis balance. *In vitro* experiments showed lack of lipid accumulation on PP5-deficient MEFs and reduced fatty-acid synthase activity due to simultaneously increased level

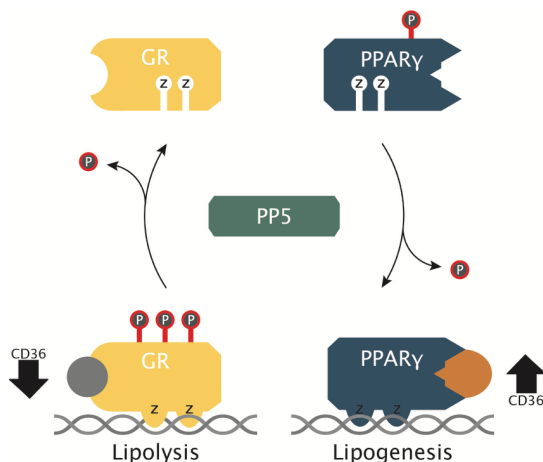


Figure 18. PP5 relevance in the lipogenesis-lipolysis axis (Adapted from Hinds *et al.* 2011). PP5 would play an elemental role in the lipogenesis-lipolysis axis by dephosphorylating GR at several serine residues and inhibiting its actions upon GR-target genes such as CD36 while also activating, through dephosphorylation, PPAR γ and activating lipogenic genes.

Introduction

of GR and reduced PPAR γ -related target genes (Hinds *et al.* 2011). Overall, the proposed model for this crosstalk is shown in Figure I8 where according to the authors PP5 would serve as an important element in lipogenesis-lipolysis axis by dephosphorylating each receptor at specific residues and antagonizing the lipolytic actions of GR while promoting those lipogenic of PPAR γ .

OBJECTIVES

The negative interaction with the JNK pathway is an action performed by different NRs, including GR, PPAR γ and LXR, and important for the pharmacological activities, anti-inflammatory and insulin sensitizing, of the agonist for these NRs. While different mechanisms have been reported to mediate GR-JNK interaction, such as direct GR-JNK interaction or MKP-1 expression, none has been demonstrated for the other two NRs, PPAR γ and LXR. Therefore, the general objective of this thesis is identifying PPAR γ and/or LXR target genes negative regulators of the JNK pathway that may be helpful for the treatment of obesity-induced IR and other inflammation-associated diseases. In addition, it is of particular interest the generation of animal models to study the NR-JNK interaction *in vivo*.

The specific objectives are:

1. To develop an *in vivo* tool to analyse the effects of the overexpression of JNK in myeloid cells, a very important cell type in early stages of *metaflammation* and consequently the development of IR.
2. To analyse whether MKP-1 mediates the insulin sensitizing activity of TZDs.
3. To analyse whether PP5 mediates the insulin sensitizing activity of LXR agonists.
4. To analyse INSIG-1 as a potential mediator in the crosstalk of PPAR γ and LXR with the JNK pathway.

MATERIALS AND METHODS

1. Cell culture

HEK293, L929, HeLa and 3T3-L1 fibroblasts were cultured in a 5% CO₂ atmosphere at 37°C in 4.5g/L D-Glucose Dulbecco's Modified Eagle Medium (DMEM) supplemented with 10% Serum (New-born Calf (NbCS) for 3T3-L1 fibroblasts and Foetal Bovine (FBS) for all other cell lines used), 0.3% Sodium Bicarbonate, 2mM L-Glutamine, 100I.U./mL Penicillin and 100µg/mL Streptomycin.

2. *In vivo* experimental models

All the protocols requiring animal manipulation have been approved by the ethical committee from University of Barcelona. All mice used in this study were in the C57BL/6J genetic background.

4.1 *Obesity-induced insulin resistance*

Male mice aged 4 to 5 weeks were challenged a 60% fat diet (HFD) (BioServe, F3282) or chow diet (SD) (BioServe, F4031) (see Annex-I for composition) *ad libitum* during periods of 10 to 12 weeks. During these period weight data was collected once per week. Initial glucose tolerance tests (GTT) were performed two days before the first challenge to the new diet and final GTT and insulin tolerance tests (ITT) were performed four and two days prior to animal euthanasia. Mice were sacrificed following the general procedure of cervical dislocation after they were anesthetized and subjected to a heart puncture and approximate 500µL of blood was collected in 1mL EDTA Tri-K tubes. Liver, adipose tissue and quadriceps muscle were also collected and frozen in liquid nitrogen. Blood was centrifuged at 1000xg for 10 minutes and the clear supernatant (plasma) was transferred to new tube. Tissue samples were stored at -80°C until further processing steps.

2.2 Glucose and insulin tolerance test

The glucose tolerance test (GTT) and insulin tolerance test (ITT) were performed in mice fasted for 6 h before injection of glucose (2g/Kg of body weight intraperitoneally) or insulin (0.5 international units/Kg of body weight, intraperitoneally), respectively. Blood was collected from the tail vein at the indicated time points and glycemia measured with an automatic glucometer (Glucocard SM, Menarini).

2.3 Nuclear receptor agonist treatments

When relevant, fifteen days before euthanasia, rosiglitazone (or dimethylformamide (DMF) diluted in PBS as vehicle) and GW3965 (or carboxymethyl cellulose (CMC) diluted in PBS as vehicle) were administered daily by oral gavage at 10 and 20 mg/Kg of body weight, respectively. For cell culture experiments, rosiglitazone and GW3965 (or DMSO as vehicle) were added at 3 and 0.25 μ M, respectively.

3. Genotyping

For genotyping purposes, ear punches were collected and incubated 2 hours at 55°C with constant agitation at 300 RPM into a thermomixer with 50 μ L of a solution with 50mM Tris-HCl pH8.0, 20mM NaCl, 1mM EDTA pH8.0, 0.1% SDS plus 60 μ g of proteinase K. Once finished, 300 μ L ddH₂O were added and incubated at 99°C for 10 minutes to inactivate the enzyme and dilute the amount of detergent used. At the end, samples were centrifuged and 2 μ L of sample were analysed by PCR. Briefly, for each reaction the following mixtures were used: MKP1 (1x commercial buffer, 5mM MgCl₂, 0.25 μ M of each primer, 1U Taq polymerase, 1 μ L DMSO and 500 μ M dNTPs), PP5 (1x commercial buffer, 5mM MgCl₂, 0.5 μ M of each primer, 1U Taq polymerase, 1 μ L DMSO and 800 μ M dNTPs), LysMCre (1x commercial buffer, 4mM MgCl₂, 0.4 μ M of

each primer, 1U Taq polymerase, 1μl DMSO and 500μM dNTPs), MKK7D-cassete (1x commercial buffer, 5mM MgCl₂, 0.5μM of each primer, 1U Taq polymerase, 1μl DMSO and 800μM dNTPs). Primers and PCR cycling parameters for each reaction can be found in Table M1 and Table M2, respectively.

Mouse colony	Sequence	
MKP1-WT	FWD	5'- CCAGCTCATTCTCCACTCATG -3'
	REV	5'- CCTGGCACAATCCTCCTAGAC -3'
MKP1-KO	FWD	5'- GAGGATATGAAGCGTTTTTCGG -3'
	REV	5'- CCTGGCACAATCCTCCTAGAC -3'
PP5-WT	FWD	5'- ACTTTGTTGCCACTGTCCCC -3'
	REV	5'- TAGCCTAAGCAGGTGCCCTC -3'
PP5-KO	FWD	5'- ACTTTGTTGCCACTGTCCCC -3'
	REV	5'- TCGTGGTATCGTTATGCGCC -3'
<i>LysMCre</i>	FWD	5'- AGGTGTAGAGAAGGCACTTAGC -3'
	REV	5'- CTAATCGCCATCTTCCAGCAGG -3'
GFP-MKK7D-cassete (positive CTL)	FWD	5'- CTAGGCCACAGAATTGAAAGATCT -3'
	REV	5'- GTAGGTGGAAATTCTAGCATCATCC -3'
MKK7D-cassete	FWD	5'- AAGTTCATCTGCACCACCG -3'
	REV	5'- TCCTTGAAGAAGATGGTGCG -3'

Table M1. Primers for genotyping the transgenic mice used in this study.

	Cycles	T (°C)	Seconds		Cycles	T (°C)	Seconds
LysMCre	1	95	240	MKP-1	1	94	300
	30	95	30		30	94	60
		55	30			50	60
		72	60			72	60
1	95	240	1	72	420		
GFP-MKK7D	1	94	300	PP5	1	94	300
	10	94	20		30	94	30
		65	15			58	30
		68	10			72	45
	28	94	15		1	72	300
		60	15				
		72	10				
	1	72	120				

Table M2. PCR parameters for the transgenic mice used in this study.

4. Primary cell culture

4.1 Bone marrow derived macrophages (BMDM).

As described by (Celada *et al.*, 1984), primary cell cultures of macrophages obtained from bone marrow were obtained by sacrificing the animal by cervical dislocation. Both legs were dissected away at the level of the hip. Then, muscle was separated from bone tissue and two cuts above and below the rotula were made to expose the bone marrow of the femur and the tibia. The bone marrow was separated from the bone by flushing in warm media with a 25G needle, disaggregated and seeded onto a new non-coated 150mm dish containing DMEM supplemented with 20% FBS, 30% L929 cell conditioned media, 0.3% Sodium Bicarbonate, 2mM L-Glutamine, 100I.U./mL Penicillin and 100µg/mL Streptomycin. After 6 days, cells were split into 60mm or 100mm non-coated dishes using 2% FBS DMEM and treatments were applied according to standardised timings.

L929 cells secrete M-CSF growth factor, necessary for the maturation of macrophages. The preparation of this specific media was done by

seeding 2×10^5 cells in a 150mm plate with 40mL of 10% FBS DMEM and culturing them for seven days. On 7th day, the media was recovered, filtered through a 0.2 μ m sterile filter, aliquot into 50mL tubes and frozen at -20°C.

4.2 Thioglycolate-elicited peritoneal macrophages.

Thioglycollate (2.5mL of a 3% solution) was injected intraperitoneally into 8-12-week-old mice 4 days before cell collection. On the harvesting day, animals were sacrificed by CO₂ inhalation and the peritoneal cavity was exposed carefully. Using a 25G needle, 10mL of free-serum Roswell Park Memorial Institute (RPMI) 1640 was injected gently into the peritoneum. Then, using a 21G needle, an approximate volume of 8mL is recovered and collected on a prechilled 50mL conical tube that is centrifuged at 4°C for 5 minutes at 300xg. The pellet was then resuspended in 1 volume RPMI, and 4 volumes of Red Blood Cell Lysis buffer pH7.4 (12mM NaHCO₃, 155mM NH₄Cl, 0.1mM EDTA) were added to eliminate all red blood cells contamination. The mixture was kept on ice for 5 minutes and then centrifuged at 300xg for 5 minutes at 4°C. The resulting pellet was resuspended in 1mL of RPMI supplemented with 10% FBS, 2mM L-Glutamine, 100I.U./mL Penicillin and 100 μ g/mL Streptomycin and cells were counted and seed onto non-coated dishes at the desired density for further treatment. After 2-3h cells were already attached to dish surface and media was changed to fresh starving 2% FCS media.

5. 3T3-L1 adipocyte differentiation

3T3-L1 fibroblasts (3×10^4 cells) were seeded on day (-4) in a 6-well plate and grown to 80-90% confluency with 10% NbCS DMEM. On day 0, media was replaced with 10% FBS DMEM supplemented with 1 μ g/mL insulin from bovine pancreas, 0.25 μ M dexamethasone and 0.5mM 3-isobutyl-1-

methylxanthine (IBMX). On day 3, media was replaced again with 10% FBS DMEM supplemented with 1µg/mL insulin from bovine pancreas. On day 5, media was replaced with 10% FBS DMEM. From day 6 to day 7, where levels of PPAR γ already reached its plateau stage, experiments performed.

6. Transient transfection of pCMV-hINSIG1-Myc

The expression plasmid pCMV-hINSIG1-6xMyc was obtained from ATCC (#88099). For transient transfection 2×10^5 cells per well were seeded in 6-well plates the day (-1). On day 0 media was changed to Opti-MEM[®] 1X media (Life Technologies) 2-3h prior transfection. Transfection cocktail was prepared according to manufacturer's instructions with some changes. Briefly, 1.6µg of plasmid (1:1 m/m with other plasmids) was mixed with 250µL of Opti-MEM[®] 1X media and 9.8µg PLUS[™] Reagent (Invitrogen). In another tube 8.1µL Lipofectamine[®] LTX (Invitrogen) were mixed with 250µL of Opti-MEM[®] 1X media. The tube containing the plasmid was added to the second tube dropwise and let rest for five minutes. Then, the mixture was spread over the 6-well plate selected wells and incubated for 24h. Cell treatments were initiated 48h post-transfection. In all experiment's plasmid expression was confirmed by immunoblotting.

7. Murine *insig-1* knock-down in 3T3-L1 fibroblasts

To prepare the retrovirus, on day (-1) 5×10^5 HEK293 cells were seeded in 100mm dishes. On day 0 calcium phosphate transfection was performed according to (Kingston RE, Chen CA, 2003) with minor changes. Briefly, 1h prior transfection, media was replaced with fresh 10% FBS DMEM. Transfection mixture was prepared with 1µg of pCAG-RTR2, 3µg of pCAG-

kGP1R, 1 μ g of pCAG-VSVG (all three were a gift from Dr. Joan Roig Lab) and 5 μ g of the selected murine shINSIG1 (TRCN0000125199, TRCN0000125200 and TRCN0000125203) plasmid combined with 50 μ L CaCl₂ 2.5M and brought up to 500 μ L volume with ddH₂O. This was added dropwise while bubbling into 500 μ L HBS 2X pH7 (50mM HEPES-NaOH pH7.0, 280mM NaCl, 1.5 mM Na₂HPO₄). After 30 minutes at room temperature, mixtures were added onto 100mm dishes and incubated at 37°C for 6h where media was completely replaced with fresh 10% FBS DMEM. On day 1, media was replaced again with 10% NbCS DMEM. On day 4, HEK293 media containing lentiviral particles was collected, filtered through 0.45 μ m sterile filter to eliminate cellular contamination and transferred to 5x10⁵ 3T3-L1 fibroblasts seeded on the previous day supplemented with 5 μ g/mL Polybrene[®] (Millipore). Fresh 10% NbCS DMEM was added to HEK293 dishes to produce more lentiviral particles to reinfect preadipocytes on day 5. On day 6, after 48h from the first infection, 3 μ g/mL puromycin was added to the media to select the infected preadipocytes. After at least 7 days with constant selective pressure, resistant cells are pooled, seeded in new plates and amplified.

8. Human *insig-1* stable transfection in HeLa

Initial steps of this protocol are equal to “Murine Insig-1 knock-down in 3T3-L1 fibroblasts” from this section (above). On day 0 transfection was performed with the same viral plasmids plus 5 μ g of the selected pCDH-CMV-3xFLAG-hINSIG1 vector (gift from Dr. Yu Li Lab) and combined with the same reagents to the same volumes. After 30 minutes at room temperature, mixtures were added onto 100mm dishes and incubated at 37°C for 6h where media was completely replaced with fresh 10% FBS DMEM. On day 1, media was replaced again with 10% FCS DMEM. On

day 4, HEK293 media containing viral particles was collected, filtered through 0.45µm sterile filter to eliminate cellular contamination and transferred to 5×10^5 HeLa cells seeded on the previous day supplemented with 5µg/mL Polybrene® (Millipore). Fresh 10% FCS DMEM was added to HEK293 dishes to produce more viral particles to reinfect HeLa cells on day 5. On day 6, after 48h from the first infection, 2µg/mL puromycin was added to the media to select the infected cells.

9. Cell extracts and immunoblotting analysis

HeLa cells were lysed with EBC lysis buffer (50mM Tris-HCl pH8.0, 170mM NaCl, 0.5% NP-40, 50mM NaF, 20mM β-glycerophosphate, 25% glycerol and added extemporaneously: 1µg/mL aprotinin, 1µg/mL leupeptin, 1mM PMSF, 0.1mM Na₃OV₄, 1mM DTT). 3T3-L1 fibroblasts or differentiated adipocytes were lysed with RIPA lysis buffer (50mM Tris-HCl pH7.4, 150mM NaCl, 1% Triton-X 100, 0.1% SDS, 0.1% sodium deoxycholate, 10mM NaF, 20mM β-glycerophosphate, 5mM EDTA, 1mM EGTA and added extemporaneously: 1µg/mL aprotinin, 1µg/mL leupeptin, 1mM PMSF, 0.1mM Na₃OV₄, 1mM DTT). After 30 minutes at 4°C whole cell extracts (WCE) were obtained by centrifugation at 13.200 rpm for 10 minutes at 4°C. Protein concentration from samples in EBC buffer was determined using Bradford reagent (BioRad), and those in RIPA buffer using Pierce Detergent Compatible Bradford Assay (Thermo Fisher) according to manufacturer's instructions.

Immunoblot analysis was carried out after separation of proteins by SDS-PAGE and transfer them to PVDF membranes using an iBlot2 system (Life Technologies). Membranes were probed with primary and secondary antibodies (Tables M3 and M4, respectively) and immunocomplexes were detected by incubating the membranes in chemiluminescence

solution (100mM Tris-HCl pH8.8, 1.25mM luminol, 2mM 4-iodophenylboronic acid, 5.3mM H₂O₂) and exposing to a X-ray film.

Antigen	Company / Reference	Dilution
phospho-JNK (Thr183, Tyr185)	Invitrogen / 700031	1:1000
phospho-JNK (Thr183, Tyr185)	BD Transduction / 642541	1:1000
JNK	Santa Cruz BT / sc-474	1:500
phospho-cJun (Ser63)	Santa Cruz BT / sc-822	1:500
Myc-tag	Santa Cruz BT / sc-40	1:1000
HA-tag	Hybridoma 15CA5	1:100
Insig1	Santa Cruz BT / sc-390504 ABCAM / ab70784	1:500 1:2000
GAPDH	Saint John's Laboratories / STJ97090	1:20000
phospho-AKT (Ser473)	Abcam / ab81283	1:1000
AKT	Santa Cruz BT / sc-1619	1:1000
β -actin	Chemicon / MAB1501R	1:2000

Table M3. Primary antibody list.

Antigen	Company / Reference	Conjugated	Dilution
Rabbit IgG (H+L)	Jackson ImmunoResearch / 711-035-152	Peroxidase	1:7000
Mouse IgG (H+L)	Jackson ImmunoResearch / 115-035-003	Peroxidase	1:7000
Mouse IgGk BP	Santa Cruz BT / sc-516102	Peroxidase	1:5000

Table M4. Secondary antibody list.

10. Enzyme-Linked Immunosorbent Assay (ELISA)

Blood insulin levels in plasma obtained from *in vivo* experiments were determined by Ultra-Sensitive Mouse Insulin ELISA Kit (Crystal Chem, 90080) following manufacturer's recommendations.

11. JNK immunocomplex assay

After selected treatments, cells were lysed with Immunocomplex Kinase Assay (ICKA) buffer (20mM HEPES-NaOH pH7.5, 10mM EGTA, 2.5mM MgCl₂, 1% NP-40, 40mM β-glycerophosphate and added extemporaneously: 1μg/mL aprotinin, 1μg/mL leupeptin, 0.5mM PMSF, 0.1mM Na₃VO₄, 1mM DTT) for 30minutes at 4°C. WCE were obtained by centrifugation at 13200 rpm for 10 minutes at 4°C. After protein quantification using Bradford reagent (BioRad), 300-500μg of WCE were immunoprecipitated. First, 1μL 50% slurry of Protein A/G resin (Nalgene), 39μL of Sepharose 50% slurry and 500μL of an anti-HA (12CA5 hybridoma) antibody were incubated at 4°C for 1h with constant rotation to obtain an enriched antibody bind to Protein A/G. Then, WCE was added and brought up to 1μg/μL with ICKA buffer. The mixture was subsequently incubated with constant rotation at 4°C for 4h. Later, three washes with PBS 1X supplemented with 1% NP-40 and 2mM Na₃VO₄ and one with Kinase buffer (20mM HEPES-NaOH pH7.5, 2.5mM MgCl₂, 20mM β-glycerophosphate and added extemporaneously 2mM DTT and 0.1mM Na₃VO₄) were performed. Approximately 1:10 of immunoprecipitated sample were aliquoted to be run later on SDS-PAGE as control and the rest was incubated with the substrate (GST-cJun) for 20 minutes at 30°C in Kinase buffer supplemented with 200μM ATP. The reaction was terminated by addition of 4X Laemli buffer and boiling the samples.

Proteins were then resolved by SDS-PAGE and immunoblotting analysis was performed.

12. Reverse transcriptase quantitative real-time PCR (RT-qPCR)

To obtain RNA, cellular pellets were lysed with TRIzol reagent (Invitrogen) following manufacturer's instructions. RNA quality was checked through an electrophoretic analysis on 1% agarose gel, reverse-transcribed with M-MLV reverse transcriptase (Invitrogen) and random hexamers. Expression of specific genes were quantified by qPCR using Power-Up SYBR Green (Applied Biosystems). Reaction mix contained 1 μ L of 1:20 diluted cDNA reaction mix, 0.3 μ M from each primer and ddH₂O up to 12.5 μ L volume. The cycle parameters are summarised in Table M5. The pairs of primers used are shown below in TableM6.

	PCR (40x cycles)			Melt Curve		
Temp (°C)	95	95	60	95	60	95
Time (s)	600	15	60	15	60	15

Table M5. List of genes and primers analysed by qPCR.

Gene	Sequence	
<i>beta-actin</i> (mouse)	FWD	5'- CTAGGCACCAGGGTGTGAT -3'
	REV	5'- CCATGTTCAATGGGGTACTT -3'
<i>gapdh</i> (human)	FWD	5'- AAGGGCTCATGACCACAGT -3'
	REV	5'- GATGCAGGGATGATGTTCTG -3'
<i>insig1</i> (mouse)	FWD	5'- AGCGTTATGCGCTGTATTGC -3'
	REV	5'- AGGCGATGGTAATCCCAAGC -3'
<i>insig2</i> (mouse)	FWD	5'- CTGTGGGAGGGGAGTAGGTC -3'
	REV	5'- TGAACGTGGGACCTACCAGA -3'

Material and methods

<i>srebp-1c</i> (mouse)	FWD	5'- CGGAAGCTGTCGGGGTAG -3'
	REV	5'- GGCCAGGAAGCAGAAGAGA -3'
<i>scd1</i> (mouse)	FWD	5'- GGCCTGTACGGGATCATACTG -3'
	REV	5'- AGCGCTGGTCATGTAGTAGA -3'
<i>chop</i> (mouse)	FWD	5'- GCCAGAATAACAGCCGGAAC -3'
	REV	5'- GACACCGTCTCCAAGGTGAA -3'
<i>fabp4</i> (mouse)	FWD	5'- GCGTGGAATTCGATGAAATCA -3'
	REV	5'- CCCGCCATCTAGGGTTATGA -3'
<i>abca1</i> (mouse)	FWD	5'- ATTCAGCTTGGTGATGCGGA -3'
	REV	5'- TGGGTCGGGAGATGAGATGT -3'
<i>il-1beta</i> (mouse)	FWD	5'- GCCCATCCTCTGTGACTCAT -3'
	REV	5'- AGGCCACAGGTATTTTGTCTG -3'
<i>il-6</i> (mouse)	FWD	5'- CCAGAGATACAAAGAAATGATGG -3'
	REV	5'- ACTCCAGAAGACCAGAGGAAAT -3'
<i>tnf alpha</i> (mouse)	FWD	5'- CAAAGGGATGAGAAGTTCCC -3'
	REV	5'- TGGTGGTTTGTACGACGT -3'
<i>dusp1</i> (mouse)	FWD	5'- CTCCACTCAAGTCTTCTTTCTCC -3'
	REV	5'- TAGGCACTGCCAGGTAC -3'
<i>slc2a4</i> (GLUT4) (mouse)	FWD	5'- GACGACGGACACTCCATCTG -3'
	REV	5'- TGCCACAATGAACCAGGGAA -3'
<i>scap</i> (mouse)	FWD	5'- ACAAGGTGACTTAGCCGAGG -3'
	REV	5'- GGGGCGAGTAACCCTTAC -3'
<i>hmgcr</i> (mouse)	FWD	5'- CATGACATTCTCCCGCCT -3'
	REV	5'- ATCCAGCGACTATGAGCGTG -3'
<i>hmgcs1</i> (mouse)	FWD	5'- ATGAAGGAATGGGGCTCGTG -3'
	REV	5'- CCAACCGTTTCCATACCCCA -3'
<i>map2k7</i> (MKK7) (human)	FWD	5'- GGGACTTCCAGTCCTTCGTC -3'
	REV	5'- GCGCTTGATGAAGCTGTGTT -3'

Table M6. List of genes and primers analysed by qPCR.

13. Statistical analysis

Data were analysed with two-tailed unpaired Student's test when two groups were compared. When having more than two groups two-way ANOVA with multiple comparison tests corrected by Tukey method was performed unless specified otherwise. Values are presented as mean \pm SEM.

RESULTS

1. To develop an *in vivo* tool to analyse the effects of the overexpression of JNK in myeloid cells, a very important cell type in early stages of *metaflammation* and consequently the development of IR.

Myeloid cells, and more especially macrophages, are a very important cell type in the development of metaflammation and, consequently, of IR. For this reason, the development of a useful tool to analyse *in vivo* how NR pathways crosstalk with the JNK proinflammatory cascade in this particular cell type would help to understand the specific role of these NRs on metaflammation and, eventually, develop of novel therapeutic approaches for the treatment of IR. For this matter, our laboratory generated a transgenic mouse in the C56BL/6J background able to express on a Cre recombinase-dependent manner a constitutively active form of the human MKK7 protein (MKK7D) (C57BL/6J-Tg(Gfp^{loxP}-MKK7D)Ccf strain, GFP-MKK7D mice from now on (see Figure R1.1 for a schema of the transgene). After transgene recombination, the expression of MKK7D promotes the activation of JNK (Lanuza-Masdeu *et al.* 2013). Using the GFP-MKK7D mice, the principal goal was to generate a new model with JNK constitutively activated in myeloid cells and analyse how this affected the mouse phenotype regarding the inflammatory response, the obesity-associated IR and, if so, its control by NRs.



Figure R1.1. The GFP-MKK7D transgene. This transgene expresses the green fluorescent protein (GFP) under the control of the constitutive CMV-β-actin promoter. The GFP transcription unit is flanked by two LoxP sites and followed by the transcription unit coding for MKK7D. Therefore, only when the GFP gene is excised by the presence of the Cre recombinase, the MKK7D is expressed (adapted from Lanuza-Masdeu *et al.* 2013).

Results

Homozygous GFP-MKK7D female mice were bred with heterozygous male mice from the strain B6.126P2-*Lyz2^{tm1(cre)}/fo*/J (LysMCre mice), also in the C56BL/6J background, that express the Cre recombinase specifically in myeloid cells. Resulting offspring were genotyped and those who presented both GFP-MKK7D and LysMCre transgenes were considered mMKK7D as they would express MKK7D in myeloid cells, and those who only had the GFP-MKK7D transgene were considered Control mice.

1.1 Effects of MKK7D expression on JNK activation and pro-inflammatory gene expression in myeloid cells.

First, we confirmed that the overexpression of MKK7D was effective in terms of an increase in MKK7D mRNA and protein expression in BMDM. Analyses of MKK7D expression and JNK activation revealed that indeed both were higher in BMDM from mMKK7D mice in comparison to those from Control littermates (FigureR1.2 A/B/E). Moreover, MKK7D expression did not limit JNK activation by other stimuli such as lipopolysaccharide (LPS) (FigureR1.2 A). Given that the increase in MKK7D expression was much higher than the effect on JNK activation, we analysed the expression of MKP-1, because it is known that activated JNK pathway triggers the expression of MKP-1 gene, as part of a negative feedback mechanism (Chu *et al.* 1996). Surprisingly, both MKP-1 mRNA and protein levels were increased in mMKK7D BMDM (FigureR1.2 C-E) confirming this possibility. In addition, a comparative expression analysis of other proinflammatory genes linked to JNK activation was performed by qPCR in total mRNA extracts from mMKK7D and Control BMDM in non- and LPS-stimulated conditions. Interestingly, basal gene expression of all genes tested, namely IL-6, IL-1 β and TNF α , was significantly higher in mMKK7D cells indicating that there was an overall activation of this pro-inflammatory pathway.

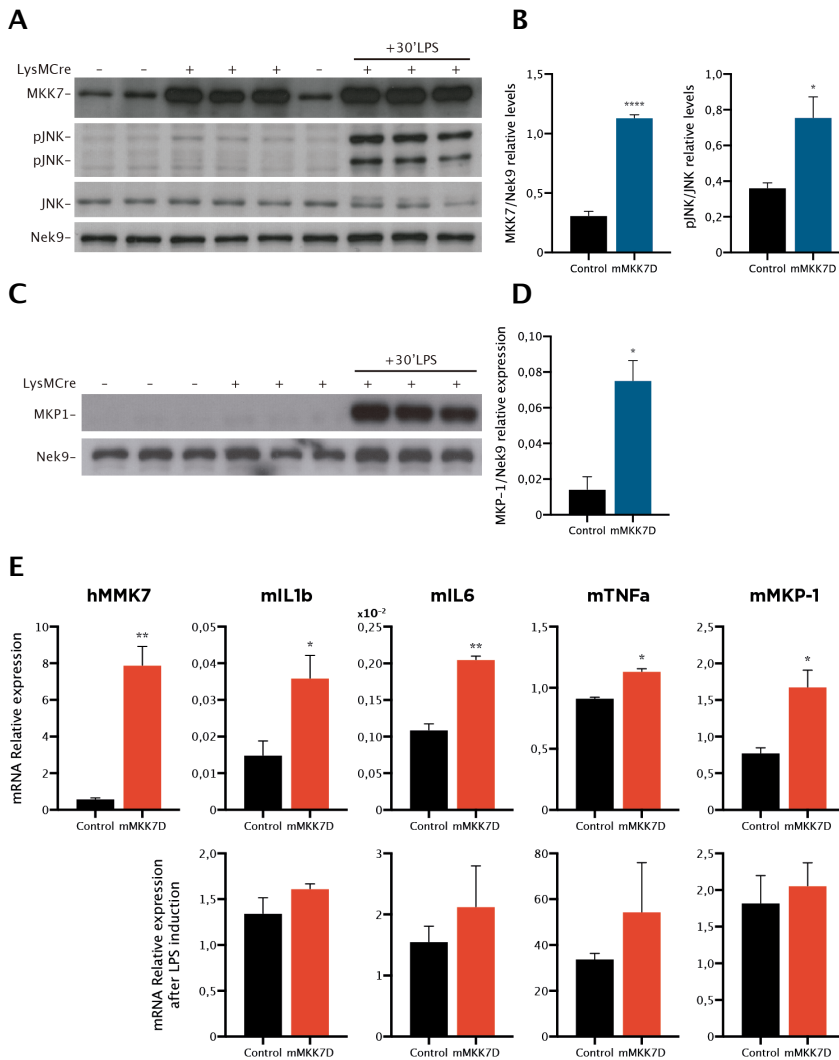


Figure R1.2. Analysis of MKK7D expression effects in Control and mMKK7D BMDM. (A) Immunoblot analysis of, from upper to lower panel, MKK7, phosphorylated/activated JNK (pJNK), JNK and Nek9 in whole protein extracts from BMDM from Control (LysMCrCre -) and mMKK7D (LysMCrCre +) mice. (B) Graphs shown relative expression of MKK7 (graph on the right) and JNK phosphorylation (graph on the left) from densitometry analysis of immunoblots shown in A. (C) Immunoblot analysis of MKP-1 (upper panel) and Nek9 (lower panel) in protein extracts from mMKK7D and Control BMDM non- or LPS-stimulated, as indicated and (D) Graphs shown relative expression of MKP-1 from densitometry analysis of immunoblots shown in C (E) Relative expression determined by qPCR analysis of the indicated genes in total RNA extracts from mMKK7D and Control BMDM non- or LPS-stimulated, as indicated. Data represent mean \pm SEM; * p <0,05, ** p <0.01, *** p <0,0001 compared to Control cells ($n \geq 3$ animals per group).

Results

Nonetheless, upon LPS stimulation these differences in gene expression between MKK7D and Control BMDM were abolished (Figure R1.2 E).

These experiments were conducted in two independent lines carrying the GFP-MKK7D transgene. Results from this second transgene line were in harmony with these presented before (not shown).

1.2 *mMKK7D mice are not protected from diet-induced obesity or IR.*

Next, we challenged mice with a HFD. For this purpose, a total amount of 30 male mice aged 4-weeks old were used for this experiment, 13 Control and 17 mMKK7D. At this age, the GTT analysis showed no differences regarding glucose tolerance between Control and mMKK7D mice (data not shown). Both groups were subdivided into two and fed either a SD or HFD for twelve weeks. During diet intervention, body weight was measured once per week. Figure R1.3 represents the weight evolution during this period in which the HFD effect was noticeable from week 7 and reached statistical significance from week 8. As can be observed, no differences in weight gain were observed between Control and MKK7D mice neither in SD nor in HFD.

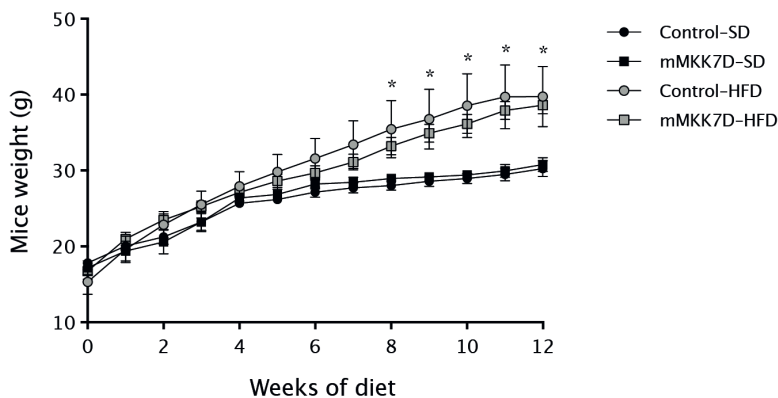


Figure R1.3. Growth curves of Control and mMKK7D mice fed a SD or HFD. The graph represents body weight (in grams) of mice along the twelve weeks of diet intervention. Data represent mean \pm SEM; * denotes statistically significant difference from Control mice in SD with $p < 0,05$. ($n \geq 4$ animals per group).

At the twelfth week of diet, animals were tested for glucose tolerance and insulin sensitivity through GTT and ITT, respectively. These analyses were performed within the same week with 48 hours of delay to allow animals to recover from test stress. Analysed results from these tests showed no significant differences between Control and MKK7D mice. Both GTT and ITT from Control and MKK7D animals presented expected values that correlated with what has been reported by many authors on this matter, that is a decrease in glucose tolerance and insulin sensitivity in HFD-fed compared to SD condition (Figure R1.4).

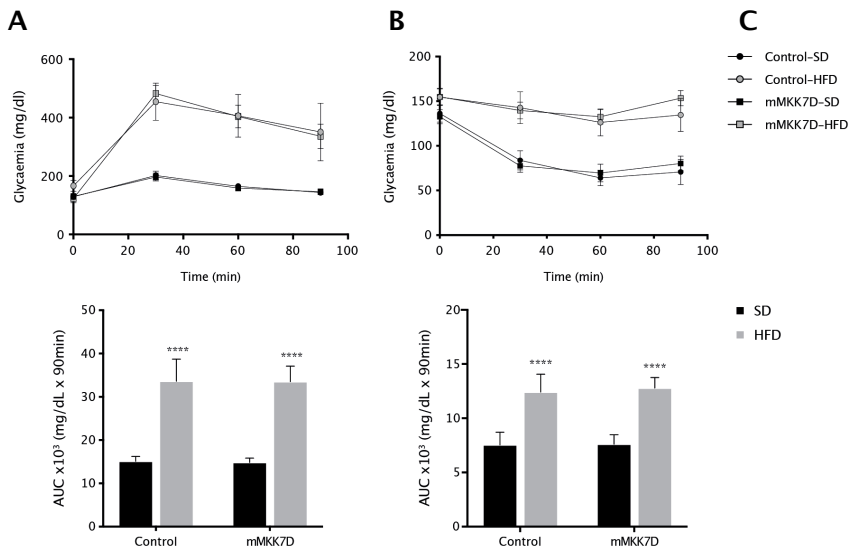


Figure R1.4. GTT and ITT performed after twelve weeks of diet intervention on Control and mMKK7D mice. (A) GTT and (B) ITT analysis of the Control and MKK7D mice on SD or HFD, as indicated. Top panels represent the glycemia at different time points after glucose (A) or insulin (B) administration, while quantification by the area under the curves (AUC) is respectively represented below. (C) Legend corresponding to parts A and B, respectively. Data represent mean \pm SEM; **** $p < 0,0001$ compared to SD ($n \geq 4$ animals per group).

2. To analyse whether MKP-1 mediates the insulin sensitizing activity of TZDs.

MKP-1 deficient mice (MKP1-KO) are protected from the development of hepatic steatosis (Flach *et al.* 2011) and of HFD-induced obesity (Wu *et al.* 2006). However, they develop HFD-induced glucose intolerance and insulin resistance (Wu *et al.* 2006). This phenotype is proposed to be caused by an inhibition of PPAR γ function due to increased MAPK-dependent phosphorylation of Ser112 of this NR. Since the insulin sensitizing action of rosiglitazone is dependent on PPAR γ and is mediated by JNK inhibition (Díaz-Delfín *et al.* 2007), we decided to analyse insulin-sensitizing action of this PPAR γ agonist in MKP-1 deficient mice. In this regards, WT and MKP1-KO mice were challenged a HFD for twelve weeks and, half of the animals from each genotype were administered rosiglitazone during the last 15 days. In parallel, a group of WT and MKP-1 KO mice were fed a SD.

2.1 MKP1-KO mice are protected from HFD-induced obesity but not from glucose intolerance or insulin resistance and are responsive to rosiglitazone.

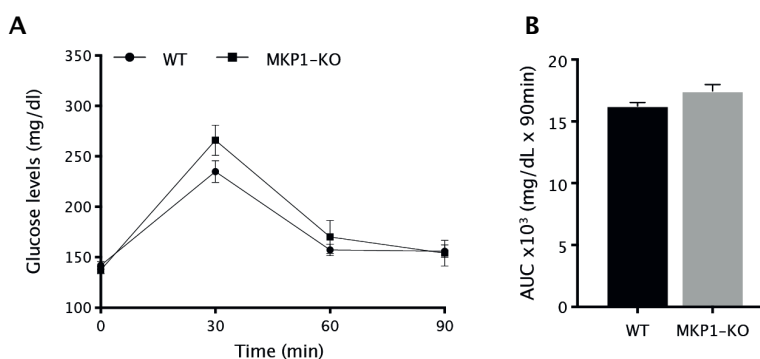


Figure R2.1. GTT analysis in 4-week old WT and MKP1-KO mice. (A) Glycemia at the indicated time points after IP injection of glucose on WT and MKP1-KO mice. (B) AUC from data shown in A. Data represent mean \pm SEM. (n=12 animals per group).

As an initial control test, both mice groups, WT and MKP1-KO, were subject of a GTT. Figure R2.1 shows that at 4-weeks of age MKP1-KO mice have a glucose tolerance similar to their WT counterparts.

On week 5 of diet, the WT group on HFD showed a significant increment in weight compared to its counterpart on SD although it was not until two weeks later that it reached statistical significance. Regarding MKP1-KO mice, their weight when fed a SD remained lower than that from WT counterparts and reached statistical significance on week 8 of diet (Figure R2.2 A). Nevertheless, when total weight gain was calculated no significant differences were found (Figure R2.2 B).

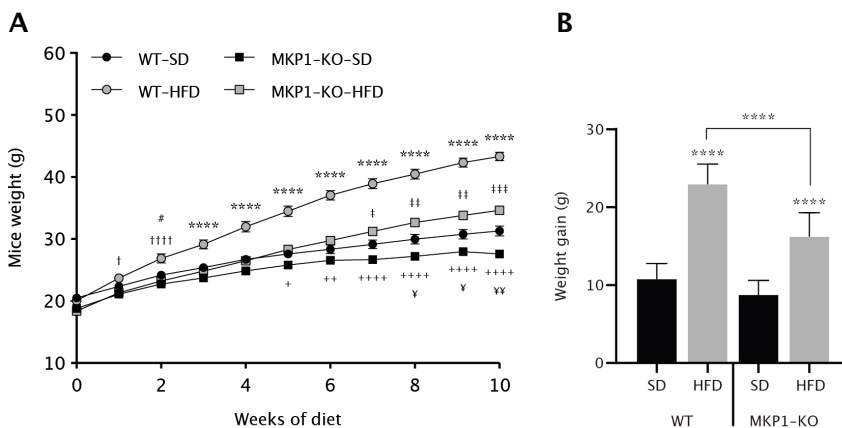


Figure R2.2. Growth curve of WT and MKP1-KO mice fed a SD or HFD. (A) Represents body weight (in grams) of mice along ten weeks of diet intervention. Weight on weeks eleventh and twelfth is not shown due to treatment-related weight variability. † denotes significant difference between WT+HFD and MKP1-KO+HFD; † $p < 0,05$, ††† $p < 0,0001$. # denotes significant difference between WT+HFD and WT+SD; # $p < 0,05$. ‡ denotes significant difference between MKP1-KO+HFD and WT+SD; ‡ $p < 0,05$, ‡‡ $p < 0,01$, ‡‡‡ $p < 0,001$. + denotes significant difference between MKP1-KO+SD and MKP1-KO+HFD; + $p < 0,05$, ++ $p < 0,01$, +++ $p < 0,0001$. ¥ denotes significant difference between WT+SD and MKP1-KO+SD; ¥ $p < 0,05$, ¥¥ $p < 0,01$. * denotes significant difference between WT+HFD and the rest groups; *** $p < 0,0001$. (B) Represents the weight gain from the initial measurement to the last after diet intervention for WT and MKP1-KO mice. * denotes significant difference between HFD and its respective SD group; *** $p < 0,0001$. Data represent mean \pm SEM ($n \geq 9$ animals per group).

Results

It is important mentioning that although we observed statistically significant differences in weight respect MKP1-KO in SD, MKP1-KO fed a HFD presented a clear leaner phenotype when compared to WT fed a HFD which reached more than 40 grams of weight at the end of the experiment. These results are in close agreement to those reported by Wu *et al.* (2006). Overall, the weight gain for WT and MKP1-KO groups is shown in Figure R2.2 B where it can be observed that both HFD groups significantly gained weight independently of its genotype, but the MKP1-KO was significantly lower.

Rosiglitazone or vehicle (DMF diluted in PBS) was administered by oral gavage once a day (10 mg/kg of weight) during the last 15 days of the experiment to half of the group of HFD-fed WT and MKP-1 KO animals. On days eleventh and thirteenth of rosiglitazone treatment, GTT and ITT were performed, and results are shown in Figure R2.3.

First, analysis from vehicle treated mice on HFD revealed that the diet-induced effect on glucose metabolism was clearly observed after twelve weeks of diet. Remarkably, WT and MKP1-KO mice on HFD showed glucose intolerance and insulin resistance to the same extent, despite that MKP1-KO mice did not develop obesity in response to the HFD. After rosiglitazone treatment, both WT and MKP1-KO mice on HFD were able to recover a normal response to insulin but retained glucose intolerance as demonstrated by ITT (Figure R2.3 B) and GTT (Figure R2.3 A), respectively. Again, no differences between WT and MKP-1 KO mice regarding the results of the rosiglitazone treatment were observed

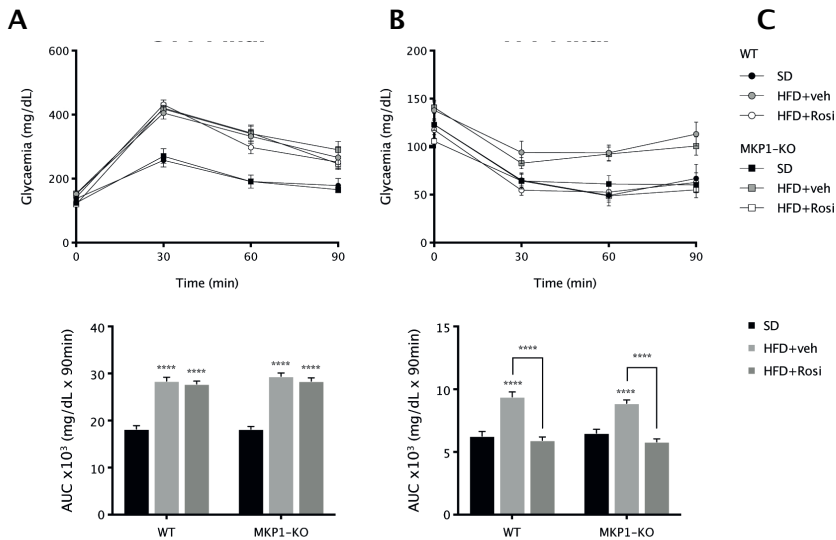


Figure R2.3. GTT and ITT performed after twelve weeks of diet intervention on WT and MKP1-KO mice. (A) GTT and (B) ITT analysis after eleven and thirteen days, respectively, of rosiglitazone (or vehicle) treatment of the WT and MKP1-KO mice on the indicated diet. Top panels represent the glycemia curves while AUC is represented in the bottom panels. (C) Legend corresponding to parts A and B. Data represent mean \pm SEM; **** $p < 0,0001$ compared to SD ($n \geq 4$ animals per group).

2.2 Rosiglitazone reduces HFD-induced hyperinsulinemia and has similar effects in *InsR* pathway in both genotypes.

At the end of the experiment and 15 minutes before euthanasia half of the mice from each group were injected IP with fast-acting human insulin in order to analyse *InsR* pathway responsiveness to insulin in different insulin target tissues. Finally, samples from blood, adipose tissue, skeletal muscle and liver were collected and analysed as follows. First, analysis of circulating insulin levels in plasma was obtained using a commercial enzyme-linked immunosorbent assay (ELISA) kit. The results shown in Figure R2.4 confirmed that after HFD intervention and vehicle treatment insulinemia significantly increased compared to animals fed a SD.

Results

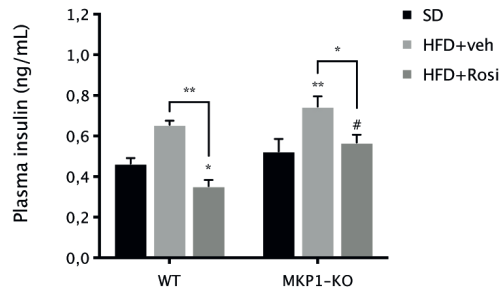


Figure R2.4. Plasma insulin analysis of WT and MKP1-KO mice after diet intervention and treatment with rosiglitazone or vehicle, as indicated. Data represent mean \pm SEM; * $p < 0,05$, ** $p < 0,01$ compared to SD from the same genotype. # $p < 0,05$ compared to the same condition from the WT group ($n \geq 4$ animals per group).

This HFD-induced hyperinsulinemia was similar for both WT and MKP-1 KO mice and correlated with the insulin-resistant phenotype shown in the ITTs (Figure R2.3 B). Also, in agreement with the results from the ITT analysis, hyperinsulinemia was reverted in response to rosiglitazone treatment, even though, circulating insulin levels were higher in MKP1-KO mice.

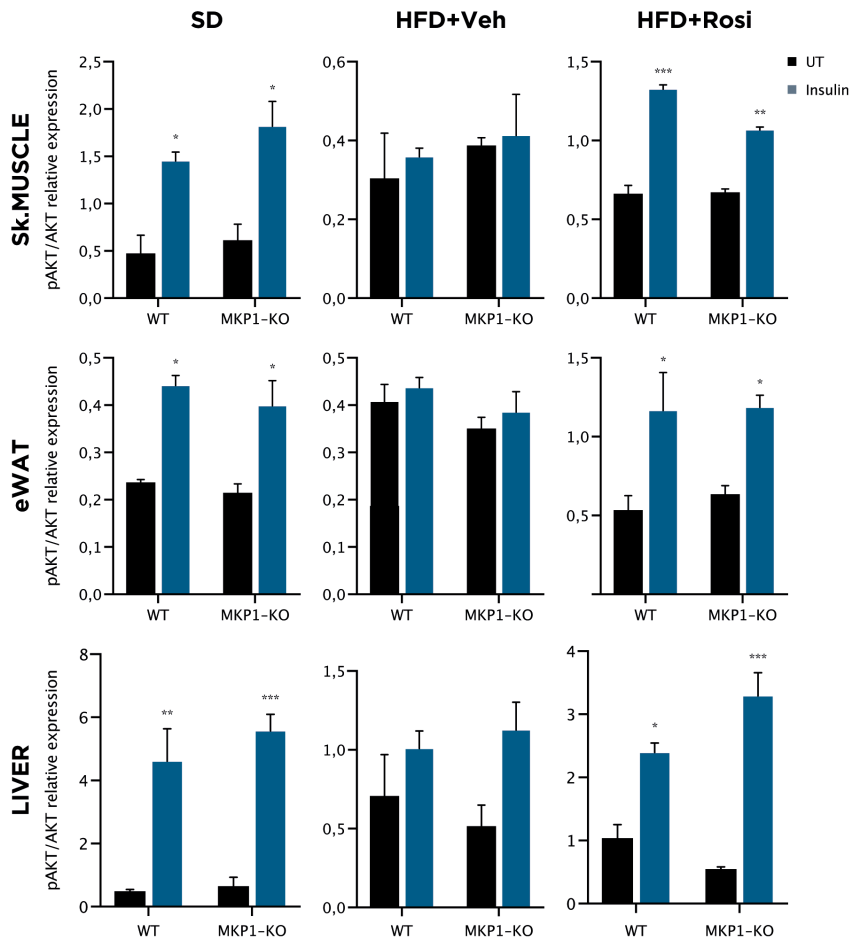


Figure R2.5. Insulin-induced activation of the InsR pathway in skeletal muscle, eWAT and liver. Bar charts represent the phospho-AKT(pAKT) versus total AKT ratio determined by immunoblotting of protein extracts of the indicated tissues from WT and MKP1-KO on the indicated diet and treatment. Data represent mean \pm SEM; * $p < 0,05$; ** $p < 0,01$, *** $p < 0,001$ compared to untreated animals from the same genotype ($n \geq 2$ animals per group).

Next, immunoblot analysis of the insulin-induced activation of InsR cascade in skeletal muscle, eWAT and liver was performed using AKT phosphorylation at Ser473 as a proxy for this response. In harmony with results from the ITT analysis presented in Figure R2.5, both WT and MKP1-KO mice fed a HFD fail to activate AKT in the three analysed tissues while insulin responsiveness was reversed by rosiglitazone treatment to almost

Results

a similar level of mice on SD. Again, WT and MKP-1 mice performed similar in these analysis in all the conditions tested indicating that MKP-1 deficiency does not interfere with the insulin sensitizing action of rosiglitazone and PPAR γ .

3. To analyse whether PP5 mediates the insulin sensitizing activity of LXR agonists.

3.1 PP5 knockout mice are not protected from diet-induced obesity, glucose intolerance or insulin resistance and did not influence LXR insulin-sensitizing action.

In this experiment, 5-week old male mice, 32 WT and 26 PP5 knockouts (PP5-KO from now on) were used. Before diet intervention, at 4 weeks of age, a GTT was performed in both mice groups. According to this test, PP5-KO mice were slightly more glucose tolerant than WT counterparts (Figure R3.1).

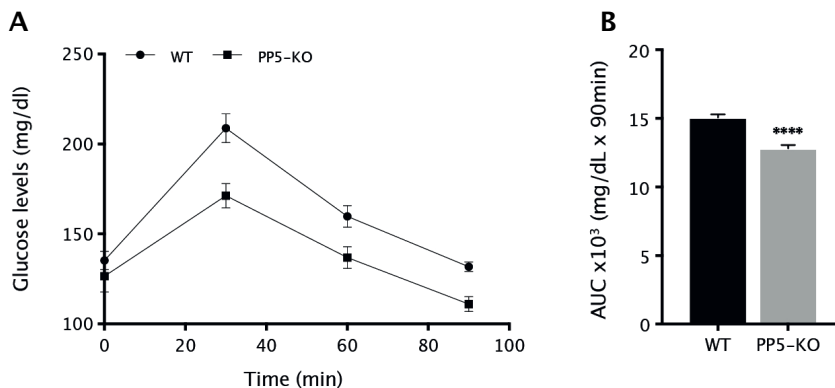


Figure R3.1. GTT in 4-week old WT and PP5-KO mice. (A) Glycemia at the indicated time points after IP injection of glucose of WT and PP5-KO mice. (B) Area under the curve (AUC) from data shown in A. Data represent mean \pm SEM; **** $p < 0,0001$. (n=12 animals per group).

Each group of mice, WT or PP5-KO was divided into two and fed either a SD or HFD for seven weeks. Body weight was measured every seven days. As shown in Figure 3.2 the diet effect was rapidly reflected in body weight

reaching statistically significant differences at four weeks of diet in both WT and PP5-KO fed a HFD compared to those fed a SD. Regardless of the genotype, HFD groups similarly increased body weight, indicating that PP5 deficiency has neither benefit nor detriment in body mass increase in response to a HFD.

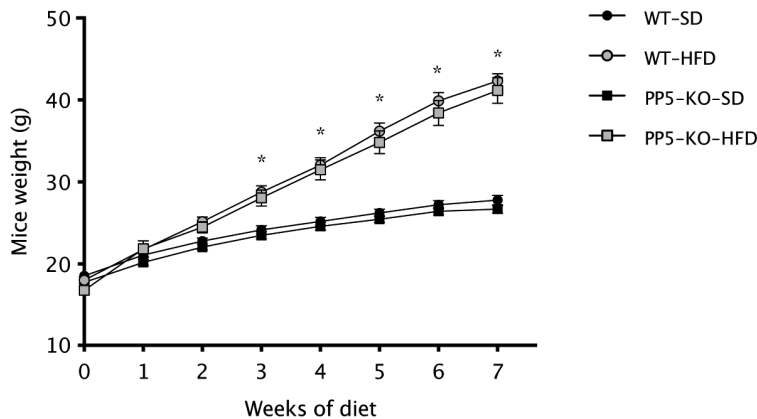


Figure R3.2. Growth curve of WT and PP5-KO mice fed a SD or HFD for seven weeks as indicated. The graph represents body weight (in grams) of mice along the seven weeks of diet intervention. Data represent mean \pm SEM; *denotes significant difference between SD and HFD groups with $p < 0,0001$. ($n \geq 12$ animals per group).

Fifteen days before euthanasia, half of the group of each genotype on HFD was treated once daily with the LXR-agonist GW3965 (GW from now on, 20mg/kg of body weight) or vehicle (CMC diluted in PBS) by oral gavage. GTT and ITT were performed at days 10 and 12 of treatment with GW, respectively. Results from GTT showed that HFD-induced glucose intolerance was alleviated by treatment with the LXR agonist, however, no significant differences between WT and PP5-KO performance in this test were observed in response to neither HFD nor GW treatment (Figure R3.3 A). Regarding insulin sensitivity, mice on HFD performed worse in the ITT than those on SD and, again, GW administration clearly improved performance in this test indicating ameliorated insulin resistance in

Results

response to GW. However, again no differences between genotypes were appreciated in response to HFD or GW treatment (Figure R3.3B).

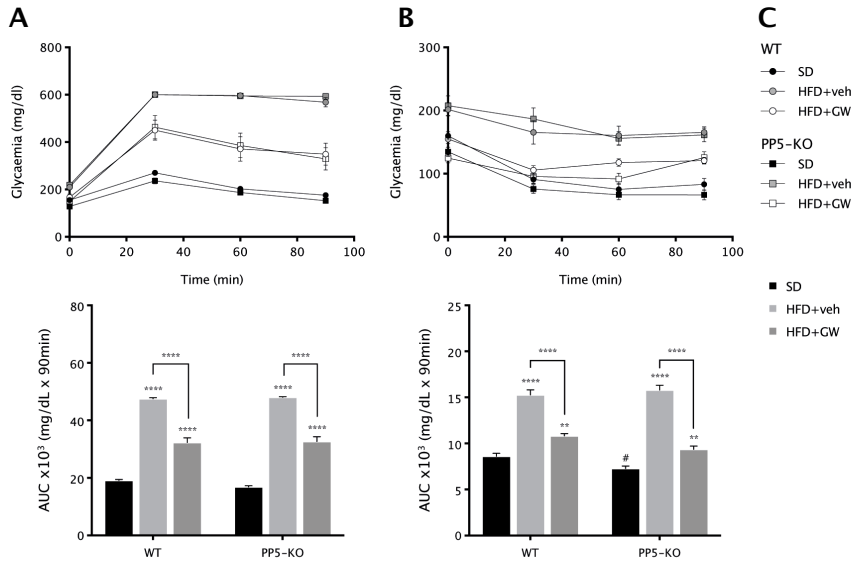


Figure R3.3. GTT and ITT performed after GW3965 or vehicle administration. (A) Corresponds to GTT data and (B) to ITT data. Top panels represent the glucose curves while quantification by the area under the curve can be found below. (C) Legend corresponding to parts A and B. Data represent mean \pm SEM; # $p < 0,05$ compared to WT littermates; ** $p < 0,01$, *** $p < 0,0001$ compared to SD or as indicated ($n \geq 4$ animals per group).

3.2 PP5 deficiency does not have a differential effect on the insulin-induced activation of the InsR cascade in insulin-target tissues.

After 14-day administration of GW, fifteen minutes before sacrifice, half of the mice of each group was treated intraperitoneally with fast-acting human insulin to evaluate the InsR cascade activation in response to this hormone by immunoblot analysis of the AKT phosphorylation on Ser473 in whole-protein extracts from insulin-target tissues such as skeletal muscle, adipose tissue and liver.

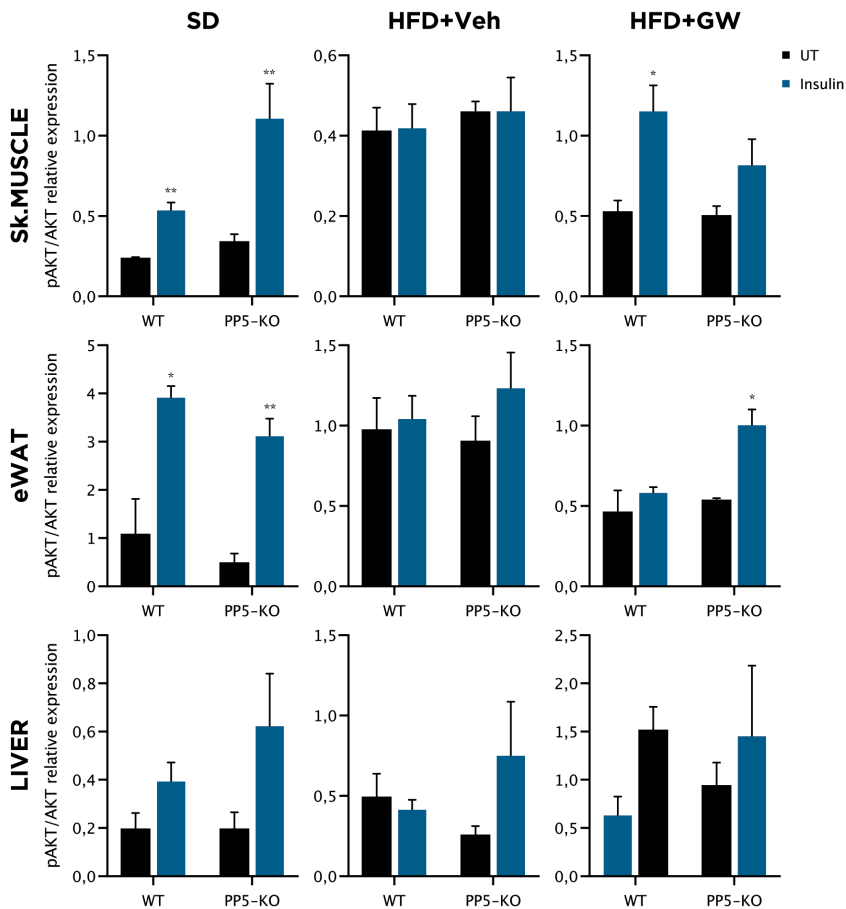


Figure R3.4. Insulin-induced activation of the InsR pathway in different tissues. Graphs represent the phospho-AKT (pAKT) versus total AKT ratio determined by immunoblot analysis of protein extracts from WT and PP5-KO in the indicated tissues and conditions. Data represent mean \pm SEM; * $p < 0,05$; ** $p < 0,01$ ($n \geq 3$ animals per group).

In SD conditions, all tissues from WT and PP5-KO mice show an increased phosphorylation/activation of AKT in response to insulin which was lost after seven weeks of HFD regardless of the genotype. This lack of insulin effect on AKT phosphorylation indicates an insulin-resistance state and agrees with the data obtained on both GTT and ITT. As shown by the ITT analysis, both genotypes recover the insulin sensitivity to a similar extent after GW treatment and, consistently, an increase insulin-induced

Results

phosphorylation of AKT was observed in the immunoblot analysis performed in these three insulin target tissues (Figure R3.4).

3.3 Obesity-induced JNK activation and its downregulation by the LXR agonist are independent of PP5.

We also analysed whether the deficiency of PP5 had any consequences in the activation of the pro-inflammatory JNK pathway of these animals after diet intervention and GW treatment. As commented before, it is well established that obesity increases the expression of pro-inflammatory markers in the adipose tissue of mice, thereby activating the JNK pathway, which in turn, interferes with responsiveness of the InsR cascade to insulin. In this context, we analysed whether GW, as an insulin-sensitizing agent, decreases the obesity-induced phosphorylation/activation of JNK. As shown in Figure R3.5 both eWAT and liver presented a significant increase of JNK phosphorylation in obese WT and PP5-KO mice which correlates with the insulin resistance observed in ITT and AKT activation analysis in different tissues. Moreover, after GW treatment the JNK phosphorylation in all cases almost decreased to SD levels, an action that is consistent with the amelioration of the obesity-associated insulin resistance. Again, both obesity-induced activation of JNK and its downregulation by GW treatment in any of these tissues was independent of PP5.

Finally, we evaluated the effect of HFD and GW treatment on the glucose transporter (GLUT)4 expression as it has been previously shown that its expression decreases by HFD (Kim *et al.* 1994; Zierath *et al.* 1997) and increases in response to LXR activation (Laffitte *et al.* 2003). Figure R3.6 shows that in both analysed tissues, eWAT and skeletal muscle, GLUT4 expression was reduced significantly after HFD intervention and regardless the genotype. However, in WT animals, GW treatment increased GLUT4 gene expression in eWAT while there was no effect in skeletal muscle.

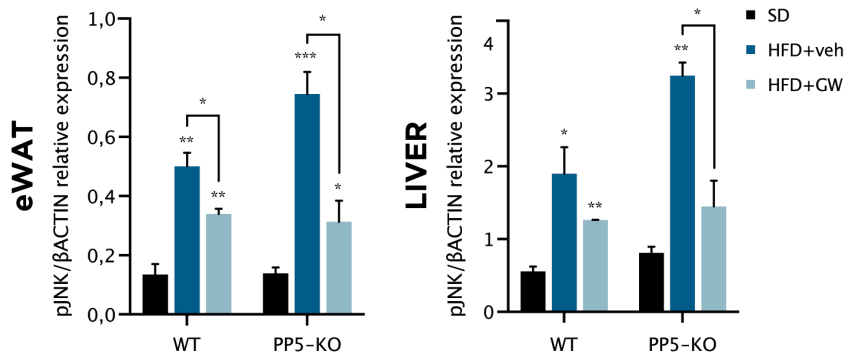


Figure R3.5. Immunoblot analysis of phosphorylated JNK in eWAT and liver of WT and PP5-KO mice in the indicated conditions. Graphs show the quantification of immunoblot analysis of JNK phosphorylation normalized to beta-actin in indicated tissues. Data represent mean \pm SEM; * $p<0,05$, ** $p<0,01$, *** $p<0,001$ ($n\geq 3$ animals per group).

Surprisingly, PP5-KO mice behaved oppositely. They did not recover any partial nor complete the level of GLUT4 in eWAT but instead, GW restored GLUT4 gene expression in skeletal muscle to a similar level to SD.

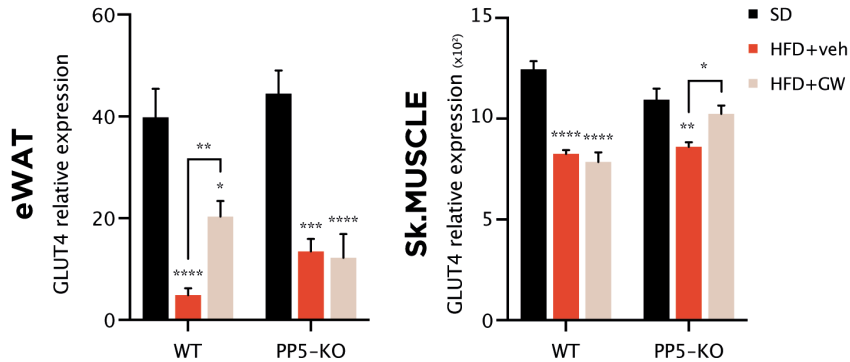


Figure R3.6. Analysis of relative GLUT4 gene expression in target tissues. Both panels show gene expression levels measured by qPCR of GLUT4, from indicated tissues, normalised to beta-actin expression levels from the same samples. Data represent mean \pm SEM; * $p<0,05$, ** $p<0,01$, *** $p<0,001$, **** $p<0,0001$ ($n\geq 3$ animals per group).

4. To analyse INSIG-1 as a potential mediator in the crosstalk of PPAR γ and LXR with the JNK pathway.

As commented in the introduction, INSIG-1 is a PPAR γ target gene (Kast-Woelbern *et al.* 2004) which has been shown to inhibit the JNK-dependent death of pancreatic β -cells in response to ERS (Chen *et al.* 2011). This relationship let us to consider INSIG-1 as a possible mediator in the TZD/PPAR γ inhibition of the JNK pathway (Díaz-Delfín *et al.* 2007).

4.1 Induction of INSIG-1 expression by PPAR γ and LXR activation.

First, we confirmed the PPAR γ -dependent expression of INSIG-1 in 3T3-L1 cell line, which expresses endogenous PPAR γ upon differentiation to adipocytes. After differentiation, these cells presented an increased expression of INSIG-1 protein and mRNA levels when incubated with the ligand for 6h (Figure R4.1). No PPAR γ -dependent expression of INSIG-1 was observed prior to differentiation, in 3T3-L1 fibroblasts (Figure R4.1 B).

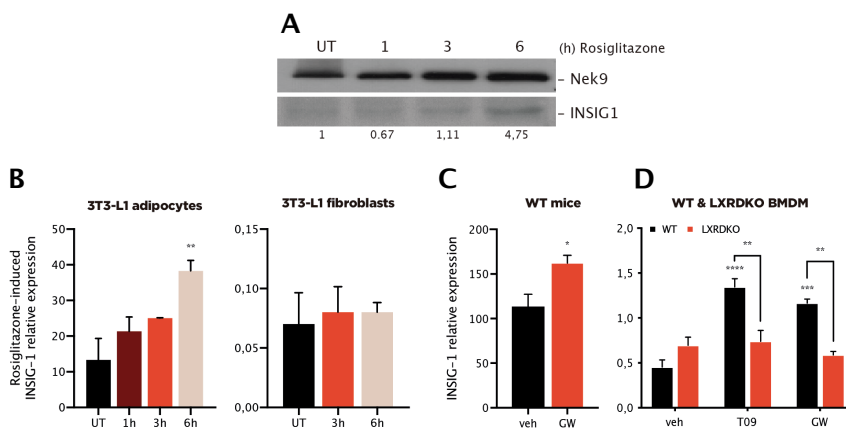


Figure R4.1. INSIG-1 expression in response to PPAR γ and LXR activation. (A) Immunoblot analysis of INSIG-1 and Nek9 in protein extracts from 3T3-L1 adipocytes treated with rosiglitazone at the indicated times. (B-D) Analysis of relative INSIG-1 to β -actin gene expression by qPCR in (B) 3T3-L1 adipocytes and fibroblasts, (C) eWAT from WT mice after GW3965 administration for 14 days and (D) WT vs. LXR-double-KO (LXRDKO) BMDM after LXR ligands (T0901317 (T09) and GW3965 (GW)) administration for 24h. Data represent mean \pm SEM (n=3); *p<0,05 **p<0,01, ***p<0,001 compared to vehicle or untreated condition.

We also analysed INSIG-1 expression in response to LXR activation in eWAT of WT mice treated with GW. In this regard, GW treatment for fourteen days resulted in increased expression of INSIG-1 in eWAT (Figure R4.1 C). Subsequently, we performed an experiment with BMDM from LXR α/β knockout (LXRDKO) mice to confirm if this activation was dependant on LXR. These results indicated that the activation of INSIG-1 by LXR agonists T0901317 and GW3965 was dependent on the presence of this NR (Figure R4.1 D).

The following step to elucidate a potential regulatory link between INSIG-1 and JNK was analyse whether INSIG-1 was able to inhibit ERS-induced JNK activation. For this purpose, 3T3-L1 fibroblasts were infected with a lentiviral vector to downregulate INSIG-1 expression by RNAi and selected. Four infected populations were obtained (M, A, B and C) where M corresponds to mock-down cells and the other three to INSIG-1 knock-down from three different INSIG-1 RNAi lentivirus. As it can be observed in Figure R4.2, basal level of INSIG-1 gene expression was effectively decreased in all three knock-down cells compared to the mock-down condition and no compensatory effect could be observed in any of the SREBP pathway target genes (INSIG-2, SREBP-1c and SCAP). However, it seems that SCD1, a target gene involved in fatty acid synthesis, presented increased expression in INSIG-1 knock-down cells although only those infected with the B lentivirus achieved statistical significance. A similar effect could be observed in genes from the cholesterol biosynthetic pathway, both HMG-CoA reductase and synthetase (HMGR and HMGS, respectively) showed an increased expression which is more evident in cells from C lentiviral infection. Regarding ABCA1, a cholesterol transporter involved in the LXR pathway, INSIG-1 knock-down induced its

Results

expression in A and B cells though this effect did not achieve statistical significance.

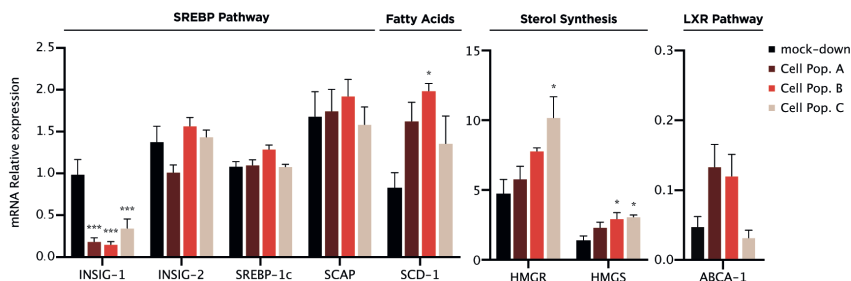


Figure R4.2. Gene expression analysis in INSIG1-KD 3T3-L1 fibroblasts by qRT-PCR. Four cell populations (mock-down, A, B and C) were isolated and tested for eight genes related to INSIG-1 according to McFarlane *et al.* (2014). Clones A to C correspond to INSIG-1 knock-down clones. Data represent mean \pm SEM; * $p < 0,05$, *** $p < 0,001$ to mock-down condition ($n \geq 2$ per group).

According to these results, B and C cells were selected to continue with the following experiments because were the ones that correlated better with the phenotype described by McFarlane *et al.* (2014). Despite the downregulation of INSIG-1 expression was effectively achieved, after the selection process, cells did not differentiate well to adipocytes, even those mock-infected. This precluded further experiments with these cells since they did not increase INSIG-1 expression in response to rosiglitazone.

4.2 INSIG-1 overexpression in HeLa cells downmodulates the JNK activation in response to different stimuli.

INSIG-1 overexpression analyses on HeLa cells were performed to assess if INSIG-1 could negatively modulate JNK activation. For that matter, WCE from vehicle- or TG-induced HeLa cells, transiently co-transfected with HA-JNK and INSIG1-myc expression plasmids, were subjected to a JNK immunocomplex assay using an anti-HA antibody to immuno-precipitate HA-JNK. Thereafter, phosphorylation of the JNK substrate, GST-c-Jun, was revealed by immunoblotting using an antibody raised against phosphorylated c-Jun on Ser-63. As shown in Figure 4.3 the TG-induction

of phosphorylation of GST-c-Jun was significantly decreased by INSIG1-myc overexpression.

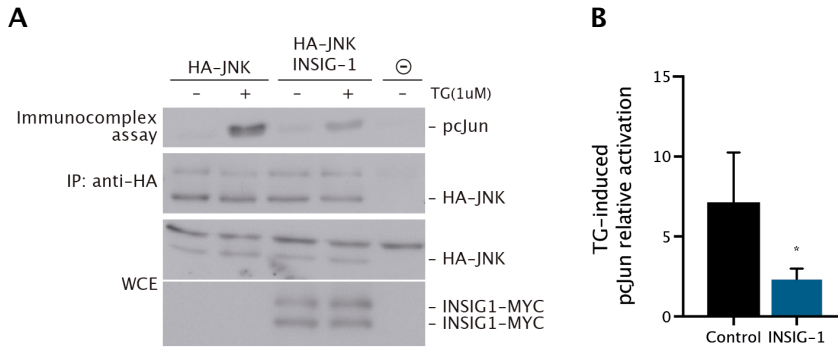


Figure R4.3. Inhibition of TG-induced JNK activation by INSIG-1 overexpression in HeLa cells. (A) post-IP and WCE immunoblots of phospho-cJun(pcJun), HA and myc. ⊖ No-transfected (B) Quantification of pcJun activation related to basal levels. Data represent mean \pm SEM; * $p < 0,05$ (n=4 per group).

Subsequently, by the use of a Flag-INSIG-1 lentiviral expression vector we generate a HeLa cell line (HeLa-Flag-INSIG-1) with a stable expression of the Flag-tag INSIG-1 and its control (HeLa-Flag). When stimulated with TG for 15 minutes cells presented a decreased activation/phosphorylation of JNK compared to same condition in mock cells (Figure R4.4 A-B). Moreover, when the same cells were stimulated with TNF α for 20 minutes the inhibitory effect of INSIG-1 overexpression on JNK activation was also observed (Figure R4.4 C-D).

Results

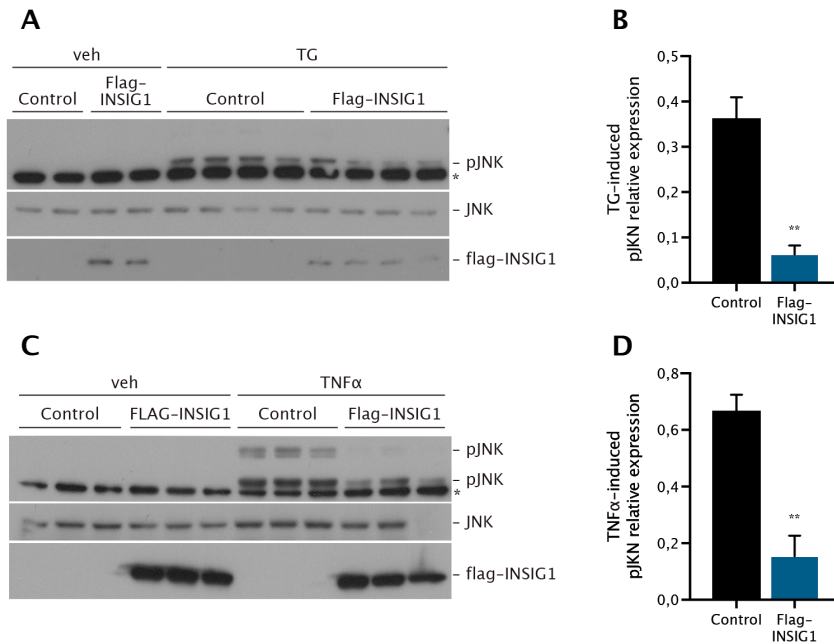


Figure R4.4. phospho-JNK (pJNK) relative activation in Control and Flag-INSIG1 HeLa cells. (A&C) WCE immunoblots of pJNK, JNK and INSIG-1. *represents unspecific band (B&D) Quantification of pJNK related to total JNK levels. Data represent mean \pm SEM; ** $p < 0,01$ ($n \geq 2$ per group).

Next, we aimed to analyse at which level along the MAPK module of the JNK pathway INSIG-1 was performing its action. For this purpose, JNK pathway was activated at the MAP3K and MAP2K level by overexpression of HA-ASK1 and MKK7D, respectively. As shown in Figure R4.5, ASK1-induced activation of JNK activation was greatly affected in HeLa-Flag-INSIG-1 in comparison to mock infected HeLa cells. Incubation with dexamethasone was used to illustrate that JNK inhibition could be accomplished in these overexpression conditions.

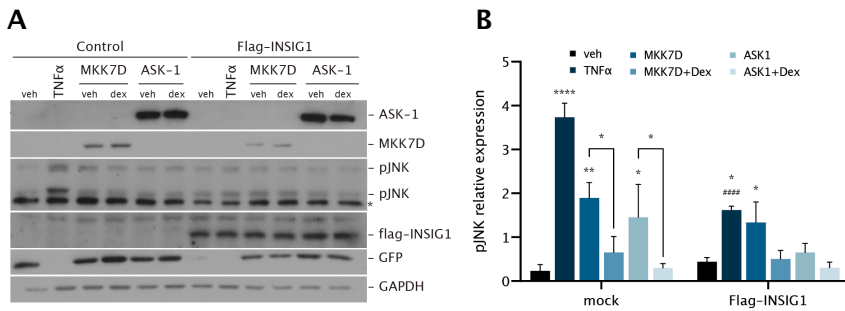


Figure R4.5. Effect of INSIG-1 overexpression on ASK-1 and MKK7D activation of JNK. Control infected HeLa and HeLa-Flag-INSIG1 cells were transiently transfected with empty, MKK7D or ASK1 expression vectors, as indicated. When relevant, 16h treatment of dexamethasone (dex) or vehicle (veh) were added. Finally, as indicated, cells were stimulated with TNF α 20 minutes before harvesting them. (A) Immunoblot analysis of, from top to bottom, ASK-1, MKK7D, pJNK, INSIG-1, GFP and GAPDH. *represents unspecific bands. (B) Quantification of pJNK normalised to GAPDH for the different conditions. Data represent mean \pm SEM; * $p < 0,05$, ** $p < 0,01$, **** $p < 0,0001$ compared to each vehicle condition, ##### $p < 0,0001$ compared to the same condition on the Control cells ($n \geq 3$ per group).

DISCUSSION

Inflammation is considered a highly regulated process crucial for the defence of the organism that recruits cells from the immune system to an infected or injured location, but it is also important for tissue repair. The size and duration of this response can have multiple outcomes from complete damage repair to cell death (Huang & Glass 2010). JNK has been considered a key player in the pro-inflammatory response. In this regard, a set of ligand-activated NRs, including PPAR γ and LXR, has been reported to inhibit JNK activation and thereby, down modulate the inflammatory response. In this dissertation, we have extended the data on this complex crosstalk by (1) developing a first-step mouse model to study the effects of JNK activation in myeloid cells, (2) concluding that rosiglitazone insulin-sensitizing action is not affected by MKP-1-deficiency, (3) confirming that PP5 is not mediating the insulin-sensitizing action of the LXR agonist GW3965, and (4) demonstrating that the PPAR γ and LXR target gene INSIG-1 is a negative regulator of the JNK cascade.

1. Developing a first-step mouse model to study the effects of JNK activation in myeloid cells.

Regarding the new mouse model constitutively overexpressing the MKK7D protein in myeloid cells (mMKK7D mice), transgene recombination effectiveness was confirmed by assessment of MKK7D overexpression at mRNA and protein level in BMDM isolated from those mice. Moreover, increased JNK activity was consistently observed in non-stimulated conditions in BMDM from mMKK7D mice compared to Control counterparts, meeting the consequences of MKK7D overexpression (Lanuzza-Masdeu *et al.* 2013). Further analysis of pro-inflammatory gene expression revealed that the overexpression of MKK7D also increased significantly IL-1 β , IL-6 and TNF α basal mRNA

expression. Therefore, these results provide a proof of concept about mouse model we aimed to develop though the level of JNK and inflammatory response activation achieved was modest.

Nonetheless, we tested whether this low but constitutive pro-inflammatory state in myeloid cells would further promote a systemic insulin resistance-related phenotype. In this regard, several studies have differentially addressed the role of myeloid JNK in obesity-associated insulin resistance (reviewed in Manieri & Sabio 2015). Among these studies, mice with myeloid-specific *jnk1* and *jnk2* genetic ablation showed to partially preserve systemic insulin sensitivity despite developing the same degree of obesity and hyperlipidemia as WT littermates (Han et al Science, 2013). Nonetheless, neither lean nor HFD-induced obese mMKK7D showed any significant difference in neither diet-induced obesity nor obesity-associated glucose intolerance or insulin resistance when compared to Control mice.

It might be possible that the inflammatory response evoked in mMKK7D mice on SD is not of enough magnitude to induce the expected phenotype. However, it is also possible that other signals in addition to the activation of the inflammatory response, such as increased insulinemia, are required to induce obesity-associated systemic insulin resistance (M. Morcillo and C. Caelles, unpublished). Regarding the former, being an enzyme-based signal transduction module, the observed activation of JNK (2 folds) was lower as it would be expected from the strong induction of MKK7D expression (4 folds). This led to the hypothesis that perhaps MKP-1 expression, the negative feedback mechanism that maintains the JNK cascade from a detrimental outcome (Wancket *et al.* 2012), could be preventing JNK activation by MKK7D in this particular cell type. This possibility is strongly supported by the

results of the MKP-1 gene expression analyses showing increased MKP-1 mRNA and protein levels already in basal conditions in mMKK7D BMDM compared to Control cells. According to our experience, this might suggest that, in contrast to pancreatic β -cells, there is a tight regulation of JNK pathway activation in myeloid cells. In pancreatic β -cells the activation of the same transgene achieved only a 2-fold increase in MKK7 expression, but this led to an almost 6-fold increase in JNK activity (Lanuza-Masdeu *et al.* 2013). Fully assessment of this hypothesis will come from studies of mMKK7D mice in a genetic background devoid of MKP-1 or, at least, with a single copy of MKP-1 gene, since the inflammation related phenotypes, such as response to septic shock, show MKP-1 gene dosage dependency (Ferré Benedito 2007).

Generation of this model would be of special interest as it might dissociate myeloid-associated systemic insulin resistance from disturbances in the adipose tissue. Of note, insulin resistance is developed in either overexpansion of adipose tissue (obesity) or limited adipose tissue development (lipodystrophy) (Bódis & Roden 2018). The achievement of a “clean” insulin resistant phenotype without the need of adding the adipose tissue-associated problems would be an interesting preclinical model where to assay drugs with “pure” insulin-sensitizing activity. Another issue that should be considered is resulting myeloid cell formation problems related to long-time active form of JNK can induce cell death and this can be considered a great risk. Huang *et al.* 2011 reported that lack of MKP-1 disrupted anti-microbial immune response and inhibited induction of regulatory T cells by downregulating TGF- β 2 production from dendritic cells. In the end, although there is a chance of developing a immunocompromised mice, there is a greater opportunity

that this animal can help evaluate and improve tissue specific JNK inhibitors *in vivo*.

In relation to the lack of differences between Control and mMKK7D mice on HFD, this is in agreement with the results of the induction of pro-inflammatory cytokines in response to LPS in BMDM, in which differences in non-stimulated conditions were abolished by stimulation.

2. Rosiglitazone insulin-sensitizing action is not affected by MKP-1-deficiency.

Pursuing the perfect anti-inflammatory drug that targets only the site of the disease without collateral damage has been a chimera for scientists. Simply, if the MAPK cascades need to be inhibited, the expression of anti-inflammatory mediators, such as MKP-1, need to increase. Usually, the block of these inflammatory cascades tends to be associated with a decrease of the inflammation and a consequently restore of body homeostasis, even though, this is not always the case. It has been shown that MKP-1 inhibitors have been beneficial in over ten cancer types where JNK-driven apoptosis pathways induced by chemotherapeutics were blocked by overexpression of this phosphatase (R. Doddareddy *et al.* 2012). On the other hand, diseases such as asthma or arthritis where MKP-1 upregulation would be beneficial to decrease the inflammatory state make its inhibitors an attractive strategy (Hopstädter & Ammit 2019). Here, we recapitulated the phenotype described by Dorfman *et al.* (1996) where MKP1-KO fed a HFD while not gaining weight as their WT littermates, became similarly glucose intolerant and insulin resistant. Authors concluded, though not proved, that the phenotype of the MKP1-KO mice was the result of impaired PPAR γ function that is, problems in adipogenesis and in the maintenance of lipid and glucose homeostasis,

including insulin-sensitizing action. Moreover, Flach *et al.* (2011) article demonstrate that MKP1-KO mice fail to activate PPAR γ target genes in hepatocytes due to increased phosphorylation of this NR at Ser112, which negatively regulates the affinity of PPAR γ for its ligands and affects its coactivator recruitment ability (Burns & Vanden Heuvel 2007). For these reasons, and due to the role of MKP-1 as a mediator of GR inhibitory action on the JNK pathway (Clark 2003), we decided to test whether MKP-1 has indeed a role in the insulin-sensitizing action of the PPAR γ ligands, TZDs. Overall, the experiments conducted to find if TZD-PPAR γ could mediate its actions on the InsR pathway through MKP1, concluded that this phosphatase is not involved in the amelioration of obesity-associated insulin resistance and argues against a PPAR γ dysfunction in MKP-1 deficient mice.

However, after rosiglitazone treatment HFD-fed MKP1-KO mice showed notably increased insulinemia compared to WT. This might suggest effects of MKP-1 deficiency in insulin secreting cells (Rosen *et al.* 2003) or in insulin clearance by the liver, among other possibilities. Therefore, deciphering the molecular causes of this phenotype will require further investigation.

3. PP5 is not mediating the insulin-sensitizing action of the LXR agonist GW3965.

Previous results from our laboratory revealed a link between PP5 and the LXR-dependent inhibition of JNK (Çavusoglu 2013). Additionally, controversial results focusing on the role of PP5 in the development of diet-induced adiposity and the associated insulin resistance have been published (Grankvist *et al.* 2013; Jacob *et al.* 2015). Therefore, we aimed to test whether PP5 could act as a mediator of the crosstalk between LXR

and JNK *in vivo* and in the context of the insulin sensitising action of LXR agonists.

The first result that we obtained from this PP5-KO model was that PP5 gene deletion had no impact on the growth and development of diet-induced obesity as all experimental groups, WT and PP5-KO, gained the same weight in response to SD and HFD irrespectively of their genotype. Average weight values reached 27g and 41g at the end of the experiment in SD- or HFD-fed groups, respectively. Moreover, as obese PP5-KO performed the same as WT littermates in GTT and ITT, we can conclude that this phosphatase does not play a role in the development of obesity-associated glucose intolerance and insulin resistance. This contrasts with results from the study of Grankvist *et al.* (2013), in which PP5-KO mice neither gained weight under HFD nor developed diet-induced insulin resistance. Given the notably differences in the obtained results, we investigated if there were any methodological differences in the experimental procedures. Mice sexual maturation is accomplished around week eight of age, so our laboratory has empirically established that diet experiments need to start around week five or weight-gain problems can arise. In that work, mice were subjected to a HFD on week eight of age which could probably mean a decreased weight gain throughout the experiment.

Regarding the insulin-sensitizing action of LXR activation by agonists such as GW3965, despite that PP5 is a LXR target gene and has an inhibitory action on the JNK pathway through its negative interaction with ASK-1, obese PP5-KO mice performed similar as WT counterpart in response to the LXR agonist, either in GTT or in ITT analysis. This was further confirmed by immunoblot analysis of extracts from relevant insulin target tissues, namely skeletal muscle, eWAT and liver directed to show

either InsR responsiveness to insulin or JNK activation. In those experiments, AKT and JNK phosphorylation/activation were evaluated, respectively, and led to the conclusion that the absence of PP5 have neither any protective nor a detrimental effect on obesity-associated insulin resistance. In addition, results of the GW treatment indicate that PP5 is has not a mediator role in the GW/LXR insulin-sensitizing action. Additionally, GLUT4 mRNA expression was evaluated as it is reported to be affected negatively by obesity (Kim *et al.* 1994; Zierath *et al.* 1997). Moreover, Laffitte *et al.* (2003) reported that GLUT4 gene expression was increased in adipose tissue, though not in skeletal muscle, in response to GW. According to our data, in WT and PP5-KO mice GLUT4 expression was similarly downregulated by obesity in both tissues. Regarding LXR activation responsiveness, while we recapitulated the described response in obese WT animals, obese PP5-KO mice showed an opposite response that is, GLUT4 expression was improved in skeletal muscle but not in eWAT. This might suggest that GW/LXR insulin sensitising action would be mediated by different tissues in WT and PP5-KO mice. Further experiments are required to clarify this issue.

4. INSIG-1 is a negative regulator of the JNK cascade.

Most of the literature on INSIG-1 is focused on its regulatory role of the cholesterol biosynthesis which is exerted through its interaction with SCAP-SREBP (Ouyang *et al.* 2020). However, other roles have started to emerge such as its ability to inhibit the JNK-dependent death of pancreatic β -cells in response to ERS (Chen *et al.* 2011). In addition, it was also demonstrated to be a PPAR γ target gene with several PPREs present in the regulatory region of its gene (Kast-Woelbern *et al.* 2004).

Discussion

Our data confirmed this issue, but PPAR γ was not the only NR that increased INSIG-1 gene expression. We also confirmed that mRNA expression of INSIG-1 was increased by LXR ligands in an LXR-dependent manner. This observation made INSIG-1 even more attractive to us because one single protein could have the control to mediate the down-modulation of JNK for both PPAR γ and LXR receptors. Our hypothesis is that SREBP1, which is a common intermediate in both pathways, could be the link that connects both NRs to INSIG-1 gene transcription activation in response to their respective agonists (Kast-Woelbern *et al.* 2004; Xu *et al.* 2016).

We have demonstrated the INSIG-1 negative interaction with the JNK pathway in transient transfection analyses in HeLa cells. These results showed that INSIG-1 overexpression significantly impaired TG-induced JNK activation. Afterward, these results were verified by the generation of a HeLa cell line with stable expression of Flag-INSIG1 achieved by lentiviral infection. In this cell line, in addition to TG, we verified that INSIG-1 expression was also able to inhibit TNF α -induced activation of JNK. This indicates that INSIG-1 is perhaps not only regulating JNK in an ERS-dependent manner but in a more general way.

Finally, the effects of co-transfecting MAP3K and MAP2K (HA-ASK1 and MKK7D, respectively) in HeLa-Flag-INSIG1 helped to identify a possible, yet to be confirmed, INSIG-1 target step for the JNK inhibition, namely ASK-1. In this regard, INSIG-1 expression blocked ASK-1-dependent activation of JNK, while it did not affect JNK activation by MKK7D. This MAP3K participates in the signal transduction to JNK from ERS stimuli (Nishitoh *et al.* 2002; Zeng *et al.* 2015) as well as from TNF α . Therefore, through interfering with ASK-1, INSIG-1 would be able to blunt JNK activation in response to TG as well as TNF α . Nonetheless, new

approaches to confirm this hypothesis are needed. In this regard, we started an INSIG-1 RNAi approach on 3T3-L1 fibroblasts that could have helped discovering more details about this interaction. However, in the process of selection the ability to induce INSIG-1 after differentiation was lost in all conditions studied and resulted in a dead end. Therefore, a new approach could lie in generating the same tool in a different background, for example HeLa cells. This would help understanding if INSIG-1 is indeed acting as a 'brake' system and therefore, when impairing its expression, stimuli-dependent JNK activation would increase. These experiments were stopped due to COVID-19 pandemics and hopefully will be resumed in the future to help clarify the exact function of INSIG-1 on JNK pathway activation.

CONCLUSIONS

- BMDM from mMKK7D mice achieve a significant increased activation of JNK due to constitutively expression of MKK7D.
- mMKK7D mice under HFD are not protected from diet-induced obesity or IR.
- MKP-1 expression is increased in mMKK7D BMDM and is a possible cause of the lack of MKK7D-dependant phenotype *in vivo*.
- MKP-1 deficient mice are protected from HFD-induced obesity but not from glucose intolerance or insulin resistance.
- MKP1-KO mice fed a HFD gain significantly more weight than its SD-fed littermates but significantly less than its WT counterparts.
- Insulin-sensitizing effects of rosiglitazone in WT and MKP1-KO mice are very similar in biochemical and molecular analyses.
- HFD-induced hyperinsulinemia is reduced by rosiglitazone in WT and MKP1-KO likewise, even though, insulin levels of MKP-1 deficient mice are higher.
- PP5-KO mice are not protected from diet-induced obesity, glucose intolerance or insulin resistance.
- GW3965 insulin-sensitizing actions were independent to PP5 deficiency *in vivo*.
- GLUT4 mRNA expression analyses revealed PP5 could be related to how the insulin sensitivity restoration is recovered in a tissue-dependant manner.
- INSIG-1 expression is accomplished by PPAR γ in 3T3-L1 adipocytes after 6h of ligand incubation.

Conclusions

- *In vivo* delivery of LXR ligands showed increased INSIG-1 expression in eWAT and completely LXR-dependant activation in BMDM from LXR α/β knockout mice after LXR ligands GW3956 and T0901317.
- JNK activation is modulated by INSIG-1 after TG or TNF α stimuli.
- ASK-1 seemed to be the upstream mediator of INSIG-1 modulation over JNK activation.

REFERENCES

- Aguirre, V., Uchida, T., Yenush, L., Davis, R., & White, M. F. (2000). The c-Jun NH2-terminal kinase promotes insulin resistance during association with insulin receptor substrate-1 and phosphorylation of Ser307. *Journal of Biological Chemistry*, **275**(12), 9047–9054.
- Ahn, N. G., Seger, R., & Krebs, E. G. (1992). The mitogen-activated protein kinase activator. *Current Opinion in Cell Biology*, **4**(6), 992–999.
- Anbalagan, M., Huderson, B., Murphy, L., & Rowan, B. G. (2012). Post-translational modifications of nuclear receptors and human disease. *Nuclear Receptor Signaling*, SAGE PublicationsSage CA: Los Angeles, CA, p. nrs.10001.
- Barak, Y., Nelson, M. C., Ong, E. S., ... Evans, R. M. (1999). PPAR γ is required for placental, cardiac, and adipose tissue development. *Molecular Cell*, **4**(4), 585–595.
- Barnes, P. J. (1998). Anti-inflammatory actions of glucocorticoids: molecular mechanisms. *Clinical Science (London, England: 1979)*, pp. 557–72.
- Barnes, P. J. (2011). Glucocorticosteroids: Current and future directions. *British Journal of Pharmacology*, **163**(1), 29–43.
- Barnes, P. J. (2010). Mechanisms and resistance in glucocorticoid control of inflammation. *The Journal of Steroid Biochemistry and Molecular Biology*, **120**(2–3), 76–85.

References

- Barr, R. K., & Bogoyevitch, M. A. (2001). The c-Jun N-terminal protein kinase family of mitogen-activated protein kinases (JNK MAPKs). *International Journal of Biochemistry and Cell Biology*, Pergamon, pp. 1047–1063.
- Bode, A. M., & Dong, Z. (2007). The functional contrariety of JNK. In *Molecular Carcinogenesis*, Vol. 46, John Wiley & Sons, Ltd, pp. 591–598.
- Bódis, K., & Roden, M. (2018). Energy metabolism of white adipose tissue and insulin resistance in humans. *European Journal of Clinical Investigation*, Blackwell Publishing Ltd. doi:10.1111/eci.13017
- Bogoyevitch, M. A. (2006). The isoform-specific functions of the c-Jun N-terminal kinases (JNKs): Differences revealed by gene targeting. *BioEssays*, John Wiley & Sons, Ltd, pp. 923–934.
- Bruna, A., Nicolàs, M., Muñoz, A., Kyriakis, J. M., & Caelles, C. (2003). Glucocorticoid receptor-JNK interaction mediates inhibition of the JNK pathway by glucocorticoids. *EMBO Journal*, **22**(22), 6035–6044.
- Brunmeir, R., & Xu, F. (2018). Functional regulation of PPARs through post-translational modifications. *International Journal of Molecular Sciences*, MDPI AG, p. 1738.
- Burns, K. A., & Vanden Heuvel, J. P. (2007). Modulation of PPAR activity via phosphorylation. *Biochimica et Biophysica Acta - Molecular and Cell Biology of Lipids*, Elsevier, pp. 952–960.

- Cargnello, M., & Roux, P. P. (2011). Activation and Function of the MAPKs and Their Substrates, the MAPK-Activated Protein Kinases. *Microbiology and Molecular Biology Reviews*, **75**(1), 50–83.
- Caunt, C. J., & Keyse, S. M. (2013). Dual-specificity MAP kinase phosphatases (MKPs): Shaping the outcome of MAP kinase signalling. *FEBS Journal*, Wiley-Blackwell, pp. 489–504.
- Çavusoglu, K. (2013). *The Crosstalk between LXR and JNK pathways: mechanisms and mediators*, Universitat Pompeu Fabra.
- Chen, K., Jin, P., He, H., Xie, Y., Xie, X., & Mo, Z. (2011). Overexpression of Insig-1 protects β cell against glucolipototoxicity via SREBP-1c. *Journal of Biomedical Science*, **18**(1), 57.
- Chen, W., Dang, T., Blind, R. D., ... Garabedian, M. J. (2008). Glucocorticoid receptor phosphorylation differentially affects target gene expression. *Molecular Endocrinology*, **22**(8), 1754–1766.
- Chu, Y., Solski, P. A., Khosravi-Far, R., Der, C. J., & Kelly, K. (1996). The mitogen-activated protein kinase phosphatases PAC1, MKP-1, and MKP-2 have unique substrate specificities and reduced activity in vivo toward the ERK2 sevenmaker mutation. *Journal of Biological Chemistry*, **271**(11), 6497–6501.
- Clark, A. R. (2007). Anti-inflammatory functions of glucocorticoid-induced genes. *Molecular and Cellular Endocrinology*, **275**(1–2), 79–97.

References

- Clark, A. R. (2003). MAP kinase phosphatase 1: A novel mediator of biological effects of glucocorticoids? *Journal of Endocrinology*, *J Endocrinol*, pp. 5–12.
- Cole, T. J., Blendy, J. A., Monaghan, A. P., ... Schütz, G. (1995). Targeted disruption of the glucocorticoid receptor gene blocks adrenergic chromaffin cell development and severely retards lung maturation. *Genes & Development*, **9**(13), 1608–21.
- Cuadrado, A., & Nebreda, A. R. (2010). Mechanisms and functions of p38 MAPK signalling. *Biochemical Journal*, Portland Press, pp. 403–417.
- Desvergne, B., & Wahli, W. (1999). Peroxisome Proliferator-Activated Receptors: Nuclear Control of Metabolism*. *Endocrine Reviews*, **20**(5), 649–688.
- Díaz Delfín, J. (2007). *Implicación de jnk en el mecanismo de acción antidiabética de las tzds/ppary*, Universitat de Barcelona.
- Díaz-Delfín, J., Morales, M., & Caelles, C. (2007). Hypoglycemic action of thiazolidinediones/peroxisome proliferator-activated receptor gamma by inhibition of the c-Jun NH2-terminal kinase pathway. *Diabetes*, **56**(7), 1865–1871.
- Dong, C., Davis, R. J., & Flavell, R. A. (2002). MAP kinases in the immune response. *Annual Review of Immunology*, Annual Reviews 4139 El Camino Way, P.O. Box 10139, Palo Alto, CA 94303-0139, USA, pp. 55–72.

- Dorfman, K., Carrasco, D., Gruda, M., Ryan, C., Lira, S. A., & Bravo, R. (1996). Disruption of the *erp/mkp-1* gene does not affect mouse development: normal MAP kinase activity in ERP/MKP-1-deficient fibroblasts. *Oncogene*, **13**(5), 925–31.
- Doza, Y. N., Cuenda, A., Thomas, G. M., Cohen, P., & Nebreda, A. R. (1995). Activation of the MAP kinase homologue RK requires the phosphorylation of Thr-180 and Tyr-182 and both residues are phosphorylated in chemically stressed KB cells. *FEBS Letters*, **364**(2), 223–228.
- Edwards, P. A., Kast, H. R., & Anisfeld, A. M. (2002). BAREing it all: The adoption of LXR and FXR and their roles in lipid homeostasis. *Journal of Lipid Research*, pp. 2–12.
- Feramisco, J. D., Goldstein, J. L., & Brown, M. S. (2004). Membrane Topology of Human Insig-1, a Protein Regulator of Lipid Synthesis. *Journal of Biological Chemistry*, **279**(9), 8487–8496.
- Ferré Benedicto, S. (2007). *Papel de la MKP-1/DUSP-1 en la acción antiinflamatoria de los glucocorticoides en ratón*, Universitat de Barcelona.
- Flach, R. J. R., Qin, H., Zhang, L., & Bennett, A. M. (2011). Loss of mitogen-activated protein kinase phosphatase-1 protects from hepatic steatosis by repression of cell death-inducing DNA Fragmentation Factor A (DFFA)-like effector C (CIDEA)/fat-specific protein 27. *Journal of Biological Chemistry*, **286**(25), 22195–22202.

References

- Frijters, R., Fleuren, W., Toonen, E. J. M., ... Alkema, W. (2010). Prednisolone-induced differential gene expression in mouse liver carrying wild type or a dimerization-defective glucocorticoid receptor. *BMC Genomics*, **11**(1), 359.
- Glass, C. K., & Ogawa, S. (2006). Combinatorial roles of nuclear receptors in inflammation and immunity. *Nature Reviews Immunology*, pp. 44–55.
- Grankvist, N., Amable, L., Honkanen, R. E., Sjöholm, Å., & Ortsäter, H. (2012). Serine/threonine protein phosphatase 5 regulates glucose homeostasis in vivo and apoptosis signalling in mouse Pancreatic islets and clonal MIN6 cells. *Diabetologia*, **55**(7), 2005–2015.
- Grankvist, N., Honkanen, R. E., Sjöholm, Å., & Ortsäter, H. (2013). Genetic disruption of protein phosphatase 5 in mice prevents high-fat diet feeding-induced weight gain. *FEBS Letters*, **587**(23), 3869–3874.
- Grygiel-Górniak, B. (2014). Peroxisome proliferator-activated receptors and their ligands: Nutritional and clinical implications - A review. *Nutrition Journal*, **13**(1), 17.
- Hinds, T. D., Stechschulte, L. A., Cash, H. A., ... Sanchez, E. R. (2011). Protein phosphatase 5 mediates lipid metabolism through reciprocal control of glucocorticoid receptor and peroxisome proliferator-activated receptor- γ (PPAR γ). *Journal of Biological Chemistry*, **286**(50), 42911–42922.

- Hoes, J. N., Jacobs, J. W. G., Verstappen, S. M. M., Bijlsma, J. W. J., & Van der Heijden, G. J. M. G. (2009). Adverse events of low- to medium-dose oral glucocorticoids in inflammatory diseases: a meta-analysis. *Annals of the Rheumatic Diseases*, **68**(12), 1833–8.
- Hoppstädter, J., & Ammit, A. J. (2019). Role of dual-specificity phosphatase 1 in glucocorticoid-driven antiinflammatory responses. *Frontiers in Immunology*, Frontiers Media S.A., p. 1446.
- Hotamisligil, G. S. (2017). Inflammation, metaflammation and immunometabolic disorders. *Nature*, Nature Publishing Group, pp. 177–185.
- Huang, G., Wang, Y., Shi, L. Z., Kanneganti, T. D., & Chi, H. (2011). Signaling by the phosphatase MKP-1 in dendritic cells imprints distinct effector and regulatory T cell fates. *Immunity*, **35**(1), 45–58.
- Huang, W., & Glass, C. K. (2010). Nuclear receptors and inflammation control: Molecular mechanisms and pathophysiological relevance. *Arteriosclerosis, Thrombosis, and Vascular Biology*, *Arterioscler Thromb Vasc Biol*, pp. 1542–1549.
- Huscher, D., Thiele, K., Gromnica-Ihle, E., ... Buttgereit, F. (2009). Dose-related patterns of glucocorticoid-induced side effects. *Annals of the Rheumatic Diseases*, **68**(7), 1119–24.
- Itoh, M., Adachi, M., Yasui, H., Takekawa, M., Tanaka, H., & Imai, K. (2002). Nuclear export of glucocorticoid receptor is enhanced by c-Jun N-terminal kinase-mediated phosphorylation. *Molecular Endocrinology (Baltimore, Md.)*, **16**(10), 2382–92.

References

- Jacob, W., Rosenzweig, D., Vázquez-Martin, C., Duce, S. L., & Cohen, P. T. W. (2015). Decreased adipogenesis and adipose tissue in mice with inactivated protein phosphatase 5. *Biochemical Journal*, **466**(1), 163–176.
- Jewell, C. M., Scoltock, A. B., Hamel, B. L., Yudt, M. R., & Cidlowski, J. A. (2012). Complex human glucocorticoid receptor dim mutations define glucocorticoid induced apoptotic resistance in bone cells. *Molecular Endocrinology*, **26**(2), 244–256.
- Kassel, O., Sancono, A., Krätzschar, J., Kreft, B., Stassen, M., & Cato, A. C. (2001). Glucocorticoids inhibit MAP kinase via increased expression and decreased degradation of MKP-1. *The EMBO Journal*, **20**(24), 7108–16.
- Kast-Woelbern, H. R., Dana, S. L., Cesario, R. M., ... Leibowitz, M. D. (2004). Rosiglitazone induction of Insig-1 in white adipose tissue reveals a novel interplay of peroxisome proliferator-activated receptor γ and sterol regulatory element-binding protein in the regulation of adipogenesis. *Journal of Biological Chemistry*, **279**(23), 23908–23915.
- Khan, S., & Wang, C. H. (2014). ER stress in adipocytes and insulin resistance: Mechanisms and significance (Review). *Molecular Medicine Reports*, **10**(5), 2234–2240.
- Kim, Y., Tomohiro, T., Iwashita, S., Tokuyama, K., & Suzuki, M. (1994). Effect of high-fat diet on gene expression of GLUT4 and insulin receptor in soleus muscle. *Biochemical and Biophysical Research Communications*, **202**(1), 519–526.

- Kubota, N., Terauchi, Y., Miki, H., ... Kadowaki, T. (1999). PPAR γ mediates high-fat diet-induced adipocyte hypertrophy and insulin resistance. *Molecular Cell*, **4**(4), 597–609.
- Kyriakis, J. M., & Avruch, J. (1990). pp54 microtubule-associated protein 2 kinase: A novel serine/threonine protein kinase regulated by phosphorylation and stimulated by poly-L-lysine. *Journal of Biological Chemistry*, **265**(28), 17355–17363.
- Kyriakis, J. M., & Avruch, J. (2001). Mammalian mitogen-activated protein kinase signal transduction pathways activated by stress and inflammation. *Physiological Reviews*, American Physiological Society, pp. 807–869.
- Kyriakis, J. M., Banerjee, P., Nikolakaki, E., ... Woodgett, J. R. (1994). The stress-activated protein kinase subfamily of c-Jun kinases. *Nature*, **369**(6476), 156–160.
- Kyriakis, J. M., & Avruch, J. (2012). Mammalian MAPK signal transduction pathways activated by stress and inflammation: a 10-year update. *Physiological Reviews*, **92**(2), 689–737.
- Laffitte, B. A., Chao, L. C., Li, J., ... Tontonoz, P. (2003). Activation of liver X receptor improves glucose tolerance through coordinate regulation of glucose metabolism in liver and adipose tissue. *Proceedings of the National Academy of Sciences of the United States of America*, **100**(9), 5419–5424.

References

- Lanuza-Masdeu, J., Isabel Arévalo, M., Vila, C., Barberà, A., Gomis, R., & Caelles, C. (2013). In vivo jnk activation in pancreatic β -cells leads to glucose intolerance caused by insulin resistance in pancreas. *Diabetes*, **62**(7), 2308–2317.
- Lee, J. C., Laydon, J. T., McDonnell, P. C., ... Young, P. R. (1994). A protein kinase involved in the regulation of inflammatory cytokine biosynthesis. *Nature*, **372**(6508), 739–746.
- Lehmann, J. M., Moore, L. B., Smith-Oliver, T. A., Wilkison, W. O., Willson, T. M., & Kliewer, S. A. (1995). An antidiabetic thiazolidinedione is a high affinity ligand for peroxisome proliferator-activated receptor γ (PPAR γ). *Journal of Biological Chemistry*, **270**(22), 12953–12956.
- Lin, H. K., Wang, L., Hu, Y. C., Altuwajri, S., & Chang, C. (2002). Phosphorylation-dependent ubiquitylation and degradation of androgen receptor by Akt require Mdm2 E3 ligase. *EMBO Journal*, **21**(15), 4037–4048.
- Manieri, E., & Sabio, G. (2015). Stress kinases in the modulation of metabolism and energy balance. *Journal of Molecular Endocrinology*, BioScientifica Ltd., pp. R12–R22.
- McFarlane, M. R., Liang, G., & Engelking, L. J. (2014). Insig proteins mediate feedback inhibition of cholesterol synthesis in the intestine. *Journal of Biological Chemistry*, **289**(4), 2148–2156.
- Medzhitov, R. (2008). Origin and physiological roles of inflammation. *Nature*, pp. 428–435.

- Moosavi, S. M., Prabhala, P., & Ammit, A. J. (2017). Role and regulation of MKP-1 in airway inflammation. *Respiratory Research*, BioMed Central Ltd., pp. 1–12.
- Moras, D., & Gronemeyer, H. (1998). The nuclear receptor ligand-binding domain: Structure and function. *Current Opinion in Cell Biology*, **10**(3), 384–391.
- Morita, K. I., Saitoh, M., Tobiume, K., ... Ichijo, H. (2001). Negative feedback regulation of ASK1 by protein phosphatase 5 (PP5) in response to oxidative stress. *EMBO Journal*, **20**(21), 6028–6036.
- Navale, A. M., & Paranjape, A. N. (2016). Glucose transporters: physiological and pathological roles. *Biophysical Reviews*, Springer Verlag, pp. 5–9.
- Nishitoh, H., Matsuzawa, A., Tobiume, K., ... Ichijo, H. (2002). ASK1 is essential for endoplasmic reticulum stress-induced neuronal cell death triggered by expanded polyglutamine repeats. *Genes and Development*, **16**(11), 1345–1355.
- Nixon, M., Andrew, R., & Chapman, K. E. (2013). It takes two to tango: Dimerisation of glucocorticoid receptor and its anti-inflammatory functions. *Steroids*, Elsevier, pp. 59–68.
- Nolan, J. J., Ludvik, B., Beerdsen, P., Joyce, M., & Olefsky, J. (1994). Improvement in Glucose Tolerance and Insulin Resistance in Obese Subjects Treated with Troglitazone. *New England Journal of Medicine*, **331**(18), 1188–1193.

References

- Ouyang, S., Mo, Z., Sun, S., Yin, K., & Lv, Y. (2020). Emerging role of Insig-1 in lipid metabolism and lipid disorders. *Clinica Chimica Acta*, Elsevier B.V., pp. 206–212.
- Overington, J. P., Al-Lazikani, B., & Hopkins, A. L. (2006). How many drug targets are there? *Nature Reviews Drug Discovery*, **5**(12), 993–996.
- Ozcan, U. (2004). Endoplasmic Reticulum Stress Links Obesity, Insulin Action, and Type 2 Diabetes. *Science*, **306**(5695), 457–461.
- Pascual-García, M., & Valledor, A. F. (2012). Biological roles of liver x receptors in immune cells. *Archivum Immunologiae et Therapiae Experimentalis*, Springer, pp. 235–249.
- Peet, D. J., Turley, S. D., Ma, W., ... Mangelsdorf, D. J. (1998). Cholesterol and bile acid metabolism are impaired in mice lacking the nuclear oxysterol receptor LXR α . *Cell*, **93**(5), 693–704.
- R. Doddareddy, M., Rawling, T., & J. Ammit, A. (2012). Targeting Mitogen-Activated Protein Kinase Phosphatase-1 (MKP-1): Structure-Based Design of MKP-1 Inhibitors and Upregulators. *Current Medicinal Chemistry*, **19**(2), 163–173.
- Reginato, M. J., Krakow, S. L., Bailey, S. T., & Lazar, M. A. (1998). Prostaglandins promote and block adipogenesis through opposing effects on peroxisome proliferator-activated receptor γ . *Journal of Biological Chemistry*, **273**(4), 1855–1858.

- Reichardt, H. M., Kaestner, K. H., Tuckermann, J., ... Schütz, G. (1998). DNA binding of the glucocorticoid receptor is not essential for survival. *Cell*, **93**(4), 531–541.
- Repa, J. J., Turley, S. D., Lobaccaro, J. M. A., ... Mangelsdorf, D. J. (2000). Regulation of absorption and ABC1-mediated efflux of cholesterol by RXR heterodimers. *Science*, American Association for the Advancement of Science, pp. 1524–1529.
- Ricote, M., & Glass, C. K. (2007). PPARs and molecular mechanisms of transrepression. *Biochimica et Biophysica Acta - Molecular and Cell Biology of Lipids*, NIH Public Access, pp. 926–935.
- Robinson-Rechavi, M., Garcia, H. E., & Laudet, V. (2003). The nuclear receptor superfamily. *Journal of Cell Science*, The Company of Biologists Ltd, pp. 585–586.
- Rocchi, S., Picard, F., Vamecq, J., ... Auwerx, J. (2001). A unique PPAR γ ligand with potent insulin-sensitizing yet weak adipogenic activity. *Molecular Cell*, **8**(4), 737–747.
- Rochette-Egly, C. (2003). Nuclear receptors: Integration of multiple signalling pathways through phosphorylation. *Cellular Signalling*, Pergamon, pp. 355–366.
- Rogatsky, I., Logan, S. K., & Garabedian, M. J. (1998). Antagonism of glucocorticoid receptor transcriptional activation by the c-Jun N-terminal kinase. *Proceedings of the National Academy of Sciences of the United States of America*, **95**(5), 2050–5.

References

- Rosen, E. D., Kulkarni, R. N., Sarraf, P., ... Spiegelman, B. M. (2003). Targeted Elimination of Peroxisome Proliferator-Activated Receptor γ in β Cells Leads to Abnormalities in Islet Mass without Compromising Glucose Homeostasis. *Molecular and Cellular Biology*, **23**(20), 7222–7229.
- Rosen, E. D., & Spiegelman, B. M. (2001). PPAR γ : A Nuclear Regulator of Metabolism, Differentiation, and Cell Growth. *Journal of Biological Chemistry*, **276**(41), 37731–37734.
- Siersbæk, R., Nielsen, R., & Mandrup, S. (2010). PPAR γ in adipocyte differentiation and metabolism - Novel insights from genome-wide studies. *FEBS Letters*, pp. 3242–3249.
- Smoak, K. a., & Cidlowski, J. a. (2004). Mechanisms of glucocorticoid receptor signaling during inflammation. *Mechanisms of Ageing and Development*, **125**(10–11), 697–706.
- Spies, C. M., Strehl, C., van der Goes, M. C., Bijlsma, J. W. J., & Buttgereit, F. (2011). Glucocorticoids. *Best Practice & Research Clinical Rheumatology*, **25**(6), 891–900.
- Steffensen, K. R., Neo, S. Y., Stulnig, T. M., ... Liu, E. T. (2004). Genome-wide expression profiling; a panel of mouse tissues discloses novel biological functions of liver X receptors in adrenals. *Journal of Molecular Endocrinology*, **33**(3), 609–622.

- Tontonoz, P., Hu, E., & Spiegelman, B. M. (1995). Regulation of adipocyte gene expression and differentiation by peroxisome proliferator activated receptor γ . *Current Opinion in Genetics and Development*, **5**(5), 571–576.
- Vanden Heuvel, J. (2009). *Nuclear Receptors: A Brief Overview*. Retrieved from http://nrresource.org/wp-content/uploads/2016/10/research_article_nr_general_lowres.pdf
- Villarroya, F., Giralt, M., & Iglesias, R. (1999). Retinoids and adipose tissues: Metabolism, cell differentiation and gene expression. *International Journal of Obesity*, Nature Publishing Group, pp. 1–6.
- Wagner, B. L., Valledor, A. F., Shao, G., ... Glass, C. K. (2003). Promoter-Specific Roles for Liver X Receptor/Corepressor Complexes in the Regulation of ABCA1 and SREBP1 Gene Expression. *Molecular and Cellular Biology*, **23**(16), 5780–5789.
- Wancket, L. M., Frazier, W. J., & Liu, Y. (2012). Mitogen-activated protein kinase phosphatase (MKP)-1 in immunology, physiology, and disease. *Life Sciences*, Pergamon, pp. 237–248.
- Wang, Z., Chen, W., Kono, E., Dang, T., & Garabedian, M. J. (2007). Modulation of glucocorticoid receptor phosphorylation and transcriptional activity by a C-terminal-associated protein phosphatase. *Molecular Endocrinology*, **21**(3), 625–634.

References

- Widmann, C., Gibson, S., Jarpe, M. B., & Johnson, G. L. (1999). Mitogen-activated protein kinase: Conservation of a three-kinase module from yeast to human. *Physiological Reviews*, American Physiological Society, pp. 143–180.
- Wu, J. J., Roth, R. J., Anderson, E. J., ... Bennett, A. M. (2006). Mice lacking MAP kinase phosphatase-1 have enhanced MAP kinase activity and resistance to diet-induced obesity. *Cell Metabolism*, **4**(1), 61–73.
- Xia, L., Liu, J., Sun, Y., ... Yin, S. (2019). Rosiglitazone improves glucocorticoid resistance in a sudden sensorineural hearing loss by promoting MAP kinase phosphatase-1 expression. *Mediators of Inflammation*, **2019**. doi:10.1155/2019/7915730
- Xu, H. F., Luo, J., Zhao, W. S., ... Bionaz, M. (2016). Overexpression of SREBP1 (sterol regulatory element binding protein 1) promotes de novo fatty acid synthesis and triacylglycerol accumulation in goat mammary epithelial cells. *Journal of Dairy Science*, **99**(1), 783–795.
- Youssef, J. A., Badr, M. Z., Youssef, J. A., & Badr, M. Z. (2013). Tissue Distribution and Versatile Functions of PPARs. In *Peroxisome Proliferator-Activated Receptors*, Humana Press, pp. 33–69.
- Yu, K., Bayona, W., Kallen, C. B., ... Lazar, M. A. (1995). Differential activation of peroxisome proliferator-activated receptors by eicosanoids. *Journal of Biological Chemistry*, **270**(41), 23975–23983.

- Zeng, T., Peng, L., Chao, H., ... Wang, G. (2015). IRE1 α -TRAF2-ASK1 complex-mediated endoplasmic reticulum stress and mitochondrial dysfunction contribute to CXC195-induced apoptosis in human bladder carcinoma T24 cells. *Biochemical and Biophysical Research Communications*, **460**(3), 530–536.
- Zierath, J. R., Houseknecht, K. L., Gnudi, L., & Kahn, B. B. (1997). High-fat feeding impairs insulin-stimulated GLUT4 recruitment via an early insulin-signaling defect. *Diabetes*, **46**(2), 215–223.
- Ziouzenkova, O., & Plutzky, J. (2008). Retinoid metabolism and nuclear receptor responses: New insights into coordinated regulation of the PPAR-RXR complex. *FEBS Letters*, FEBS Lett, pp. 32–38.

ANNEX-I

1. Diet nutritional profile sheet for standard diet



Delivering Solutions™

◆ Nutritional ◆ Enrichment ◆ Medicated ◆ Special Needs

Product# F4031 - Mouse Diet, Control for F1850/F3282, 1/2" Pellets

Proximate Profile

Protein	%	20.5
Fat	%	7.2
Fiber	%	0.0
Ash	%	3.5
Moisture	%	<10
Carbohydrate	%	61.6

Caloric Profile

Protein	kcal/gm	0.82
Fat	kcal/gm	0.64
Carbohydrate	kcal/gm	2.46
Total	kcal/gm	3.93

Amino Acids

Alanine	gm/kg	5.3
Arginine	gm/kg	7.3
Aspartic Acid	gm/kg	12.8
Cystine	gm/kg	0.6
Glutamic Acid	gm/kg	40.6
Glycine	gm/kg	4.9
Histidine	gm/kg	5.5
Isoleucine	gm/kg	11.0
Leucine	gm/kg	16.6
Lysine	gm/kg	14.8
Methionine	gm/kg	7.1
Phenylalanine	gm/kg	8.9
Proline	gm/kg	20.5
Serine	gm/kg	11.4
Threonine	gm/kg	8.7
Tryptophan	gm/kg	2.2
Tyrosine	gm/kg	11.4
Valine	gm/kg	13.0

Carbohydrates

Monosaccharides	gm/kg	0.6
Disaccharides	gm/kg	243
Polysaccharides	gm/kg	368

Fatty Acids

C18:2 Linoleic	gm/kg	7.1
C18:3 Linolenic	gm/kg	0.7
Total Saturated	gm/kg	27
Total Monounsaturated	gm/kg	32
Total Polyunsaturated	gm/kg	7.8

Minerals

Calcium	gm/kg	5.6
Chloride	gm/kg	0.86
Copper	mg/kg	3.6
Chromium	mg/kg	0.41
Fluoride	mg/kg	11.0
Iodine	mg/kg	0.31
Iron	mg/kg	40.8
Magnesium	gm/kg	0.49
Manganese	mg/kg	46.7
Phosphorus	gm/kg	5.8
Potassium	gm/kg	5.6
Selenium	mg/kg	0.21
Sodium	mg/kg	571
Sulfur	mg/kg	668
Zinc	mg/kg	21.6

Vitamins

Choline	mg/kg	1005
Folic Acid	mg/kg	0.75
Niacin	mg/kg	15.0
Pantothenic Acid	mg/kg	5.5
Pyridoxine	mg/kg	4.1
Riboflavin	mg/kg	2.3
Thiamin	mg/kg	3.0
Vitamin A	IU/kg	3162
Vitamin B ₁₂	mcg/kg	40
Vitamin D ₃	IU/kg	1000
Vitamin E	IU/kg	23.1
Vitamin K ₃ (Menadione)	mg/kg	0.52

Ingredients

Cornstarch, Sucrose, Casein, Maltodextrin, Lard, Mineral Mix, Vitamin Mix, DL Methionine, Choline Chloride

These are typical amounts of nutrients calculated from available information. Actual assay results may vary. For more information contact Jaime Lecker, Ph.D. Phone: 800-996-9908 ext. 112 (U.S. and Canada) 908-284-2155 (International) Email: jlecker@bio-serv.com.

Revised Date: 10/11

ISO 9001:2008 Certified
3 Foster Lane, Suite 201, Flemington, NJ 08822 • Toll-Free: 800-996-9908 (U.S. & Canada)
Phone: 908-284-2155 (International) • Fax: 908-284-4753 • Web: www.bio-serv.com

Copyright© 2015 Bio-Serv
All Rights Reserved

2. Diet nutritional profile sheet from high fat diet



Delivering Solutions™

◆ Nutritional ◆ Enrichment ◆ Medicated ◆ Special Needs

Product# F3282 - Mouse Diet, High Fat, Fat Calories (60%), 1/2" Soft Pellets, 5 kg/Box
 Product# S3282 - Mouse Diet, High Fat, Fat Calories (60%), 1/2" Soft Pellets, 5 kg/Box - Sterile

Proximate Profile

Protein	%	20.5
Fat	%	36.0
Fiber	%	0.0
Ash	%	3.5
Moisture	%	<10
Carbohydrate	%	35.7

Caloric Profile

Protein	kcal/gm	0.82
Fat	kcal/gm	3.24
Carbohydrate	kcal/gm	1.43
Total	kcal/gm	5.49

Amino Acids

Alanine	gm/kg	5.3
Arginine	gm/kg	7.3
Aspartic Acid	gm/kg	12.8
Cystine	gm/kg	0.6
Glutamic Acid	gm/kg	40.6
Glycine	gm/kg	4.9
Histidine	gm/kg	5.5
Isoleucine	gm/kg	11.0
Leucine	gm/kg	16.6
Lysine	gm/kg	14.8
Methionine	gm/kg	7.1
Phenylalanine	gm/kg	8.9
Proline	gm/kg	20.5
Serine	gm/kg	11.4
Threonine	gm/kg	8.7
Tryptophan	gm/kg	2.2
Tyrosine	gm/kg	11.4
Valine	gm/kg	13.0

Carbohydrates

Monosaccharides	gm/kg	1.3
Disaccharides	gm/kg	146
Polysaccharides	gm/kg	200

Fatty Acids

C18:2 Linoleic	gm/kg	36.6
C18:3 Linolenic	gm/kg	3.6
Total Saturated	gm/kg	141
Total Monounsaturated	gm/kg	162
Total Polyunsaturated	gm/kg	40.2

Minerals

Calcium	gm/kg	5.6
Chloride	gm/kg	0.86
Copper	mg/kg	3.6
Chromium	mg/kg	0.41
Fluoride	mg/kg	11.0
Iodine	mg/kg	0.31
Iron	mg/kg	40.8
Magnesium	gm/kg	0.49
Manganese	mg/kg	46.7
Phosphorus	gm/kg	5.8
Potassium	gm/kg	5.6
Selenium	mg/kg	0.21
Sodium	mg/kg	571
Sulfur	mg/kg	668
Zinc	mg/kg	21.6

Vitamins

Choline	mg/kg	1148
Folic Acid	mg/kg	0.75
Niacin	mg/kg	15.0
Panthenic Acid	mg/kg	5.5
Pyridoxine	mg/kg	4.1
Riboflavin	mg/kg	2.3
Thiamin	mg/kg	3.0
Vitamin A	IU/kg	3162
Vitamin B ₁₂	mcg/kg	40
Vitamin D ₃	IU/kg	1000
Vitamin E	IU/kg	25.7
Vitamin K ₃ (Menadione)	mg/kg	0.52

Ingredients

Lard, Casein, Maltodextrin, Sucrose, Mineral Mix,
 Vitamin Mix, DL-Methionine, Choline Chloride

These are typical amounts of nutrients calculated from available information. Actual assay results may vary. For more information contact Jaime Lecker, Ph.D. Phone: 800-996-9908 ext. 112 (U.S. and Canada) 908-284-2155 (International) Email: jlecker@bio-serv.com.

Revised Date: 1/11

ISO 9001:2008 Certified
 3 Foster Lane, Suite 201, Flemington, NJ 08822 • Toll-Free: 800-996-9908 (U.S. & Canada)
 Phone: 908-284-2155 (International) • Fax: 908-284-4753 • Web: www.bio-serv.com

Copyright© 2015 Bio-Serv
 All Rights Reserved

